The final publication is available at

https://doi.org/10.1111/tpj.13905

Additional Information

DR PASCAL RATET (Orcid ID : 0000-0002-8621-1495)

Article type   : Original Article

Lotus japonicus NOOT-BOP-COCH-LIKE1 is essential for nodule, nectary, leaf and flower development

Kévin Magne[1,2], Jeoffrey George[1,2,*], Ana Berbel Tornero[3], Blandine Broquet[1,2], Francisco Madueño[3], Stig Uggerhøj Andersen[4] and Pascal Ratet[1,2,§]

[1] Institute of Plant Sciences Paris-Saclay IPS2, CNRS, INRA, Université Paris-Sud, Université Evry, Université Paris-Saclay, Bâtiment 630, 91405 Orsay, France

[2] Institute of Plant Sciences Paris-Saclay IPS2, Paris Diderot, Sorbonne Paris-Cité, Bâtiment 630, 91405, Orsay, France

[3] Instituto de Biología Molecular y Celular de Plantas, CSIC-UPV, Universidad Politécnica de Valencia, CPI Edificio 8E, Avenida de los Naranjos s/n, Valencia 46022, Spain

[4] Department of Molecular Biology and Genetics, Centre for Carbohydrate Recognition and Signaling, Aarhus University, Gustav Wieds Vej 10, Aarhus C DK-8000, Denmark

[*] Present address: The Sainsbury Laboratory, Norwich Research Park, Norwich, NR4 7UH, United Kingdom

[§] Denotes corresponding authorship e-mail: pascal.ratet@ips2.universite-paris-saclay.fr; pascal.ratet@cnrs.fr telephone: +33 169 153 377

Running head: *NBCL* roles in Lotus development

Key words: *NOOT-BOP-COCH-LIKE* genes, determinate nodule, nodule identity, nectary glands, flower development, leaf patterning, *Lotus japonicus,* organogenesis.

ABSTRACT

The *NOOT-BOP-COCH-LIKE* (*NBCL*) genes are orthologs of *Arabidopsis thaliana BLADE-ON-PETIOLE1/2*. *NBCLs* are developmental regulators essential for plant shaping mainly through the regulation of organ boundaries, the promotion of lateral organ differentiation and the acquisition of organ identity. In addition to their roles in leaf, stipule and flower development, *NBCLs* are required for maintaining the identity of indeterminate nitrogen fixing nodules with persistent meristems in legumes. In legume forming determinate nodules without persistent meristem, the roles of the *NBCL* genes are not known. We thus investigated the role of the *Lotus japonicus LjNOOT-BOP-COCH-LIKE1* (*LjNBCL1*) in determinate nodule identity and studied its functions in aerial organ development using *LORE1* insertional mutants and RNAi-mediated silencing approaches. In *Lotus, LjNBCL1* is involved in leaf patterning and participates in the regulation of axillary outgrowth. Wild-type *Lotus* leaves are composed of five leaflets and possess a pair of nectaries at the leaf axil. Legumes such as pea and *Medicago* have a pair of stipules at the base of their leaves, rather than nectaries. In *Ljnbcl1*, nectaries development is abolished, demonstrating that nectaries and stipules share a common evolutionary origin. In addition, ectopic roots arising from nodule vascular meristems and re-organization of the nodule vascular bundle vessels were observed on *Ljnbcl1* nodules. This demonstrates that *NBCL* functions are conserved in both indeterminate and determinate nodules through the maintenance of nodule vascular bundle identity. In contrast to their roles in floral patterning described in others plants, *LjNBCL1* appears essential for both secondary inflorescence meristem and floral meristem development.

INTRODUCTION

The *NOOT-BOP-COCH-LIKE* (*NBCL*) genes, contain BTB/POZ (BROAD COMPLEX, TRAMTRACK and BRICK A BRACK/POXVIRUSES and ZINC FINGER) and ANKYRIN repeat domains and encode co-transcriptional factors involved in the gene regulatory network required for plant boundaries regulation (Aida and Tasaka, 2006a,b; Zadnikova and Simon, 2014; Hepworth and Pautot, 2015; Wang *et al.,* 2016). These *NBCL* genes play important roles in stipule, leaf and flower patterning and identity (Yaxley *et al*., 2001; Ha *et al*., 2003, 2004, 2007; Hepworth *et al*., 2005; Norberg *et al*., 2005; Xu *et al*., 2010; Couzigou *et al.*, 2012; Khan *et al*., 2012; Khan *et al*., 2015; Tavakol *et al*., 2015; Jost *et al*., 2016) as well as in the abscission process (McKim *et al*., 2008; Wu *et al.*, 2012; Couzigou *et al*., 2016). *NBCL* genes were in addition recruited to the nodules of legume plants to determine their identity

(Ferguson and Reid, 2005; Couzigou *et al.*, 2012). The *NBCL* gene clade includes genes orthologous to *Arabidopsis thaliana* (*A. thaliana*) *AtBLADE-ON-PETIOLE1* and *AtBLADE-ON-PETIOLE2 (AtBOP1, AtBOP2), Medicago truncatula (M. truncatula) MtNODULE-ROOT1* (*MtNOOT1*), *Pisum sativum* (*P. sativum*) *PsCOCHLEATA1* (*PsCOCH1*) and *Hordeum vulgare* (*H. vulgare*) *HvUniculme4* (*Cul4*) and *HvLaxatum-a* (*Lax-a*). Known *nbcl* mutants exhibit altered floral organ number, organ modification and homeosis of reproductive organs.

Legume plants from the Fabaceae family belong to the Rosideae, one of the rare clades predisposed to establish symbiosis with nitrogen fixing rhizobia (Soltis *et al.,* 1995; Werner *et al.*, 2014). This symbiosis takes place in the nodules. Legumes in the tribes Trifolieae and Fabeae form indeterminate nodules characterized by the presence of a persistent apical/central meristematic zone (Nodule Central Meristem, NCM, Franssen *et al.*, 2015) and peripheral vasculature ontologically related to roots (Ferguson and Reid, 2005; Couzigou *et al.*, 2012) because they possess a root apical meristem-like meristematic zone called the nodule vascular meristem (NVM, Franssen *et al.*, 2015). Determinate nodules are found in the tribes Phaseoleae and Loteae. They display subtle differences in terms of organogenesis and nodule organization and do not possess a persistent NCM (Corby, 1988; Guinel, 2009). In contrast to the well documented plant-bacteria recognition and infection processes as well as the *de novo* organogenesis and functioning of the nodule (Oldroyd and Downie 2008; Oldroyd, 2013; Udvardi and Poole, 2013; Suzaki *et al.*, 2015), the mechanisms underlying the acquisition and preservation of the nodule identity as well as the maintenance of the different meristematic zones present in the nodule remain poorly described. Nodule identity studies were initiated with the studies of the *P. sativum Pscochleata1* (*Pscoch1*) and *M. truncatula Mtnodule-root1* (*Mtnoot1*) *noot-bop-coch-like (nbcl)* mutants, affected in the maintenance of nodule identity (Ferguson and Reid, 2005; Couzigou *et al.*, 2012). These mutants are characterized by the emergence of root-like structures from the NVM (VandenBosch *et al.*, 1985; Akasaka *et al.*, 1998; Voroshilova *et al.,* 2003; Ferraioli *et al.*, 2004; Ferguson and Reid, 2005; Sinharoy and DasGupta, 2009; Couzigou *et al.*, 2012; Couzigou and Ratet, 2015). In indeterminate nodules, the role of these two genes is to repress the root identity of NVM (Couzigou *et al.*, 2012).

To address the role of *NBCL* genes in determinate nodules, we studied the role of the single copy *Lotus japonicus* gene *LjNOOT-BOP-COCH-LIKE* (*LjNBCL1*; Couzigou *et al.,* 2016), orthologous to *MtNOOT1*. Our study revealed that *Lj*NBCL1 functions are conserved in this species for the maintenance of the *L. japonicus* determinate nodule identity. Furthermore, we found that *Lj*NBCL1 also plays essential roles in *L. japonicus* vegetative and reproductive development. We demonstrate that *Lj*NBCL1 is involved in the regulation of compound leaf complexity, in the formation of nectary glands, in flower development, as well as in secondary inflorescence meristem development and in the promotion of flower meristem determinacy.

RESULTS

LjNBCL1 is constitutively expressed in roots and induced during nodulation

Expression studies were performed to determine whether *LjNBCL1* participates in nodule development in *L. japonicus*. *LjNBCL1* gene expression was measured in the root apical meristem (RAM), the root and in determinate nodules throughout nodulation, using *Mesorhizobium loti* (*M. loti*) strain NZP-2235 as symbiotic partner (Jarvis *et al.* 1982).

LjNBCL1 is constitutively expressed in non-inoculated *L. japonicus* roots and its expression in the RAM was detected at very low level. In primary root, two days post-inoculation (dpi), the level of *LjNBCL1* gene expression is slightly induced compared to its level in non-inoculated roots. At 5 dpi, when nodule primordia are visible, *LjNBCL1* gene expression increased. At 8 dpi, in nodules, its expression reached a maximum and at 12 dpi its expression started to decrease. From 16 dpi to 20 dpi, *LjNBCL1* gene expression seemed to stabilize (Figure 1a). This pattern of expression is consistent with the *LjNBCL1* gene expression profile obtained from the *Lotus japonicus* Gene Expression Atlas (https://ljgea.noble.org/v2/; Figure S1).

To better understand the kinetics of *LjNBCL1* expression during nodulation, its expression was compared to the expression of symbiotic marker genes known to be sequentially induced during the symbiotic process. *LjNODULE INCEPTION* (*LjNIN*), *LjEARLY NODULINE40-1* (*LjENOD40-1*), *LjLEGHEMOGLOBIN2* (*LjLEGH2*) and *LjADENYLATE ISOPENTHENYL TRANSFERASE3 (LjIPT3)* are induced from 2 dpi (Figure 1b). From 2 dpi to 8 dpi, *LjNBCL1* gene expression is induced and its gene expression kinetic is similar to the one of *LjIPT3*. After 8 dpi, by contrast to *LjIPT3* expression level which

continues to increase in nodules, *LjNBCL1* gene expression remains lower (Figure 1b). The early induction of *LjNBCL1* and its maintenance in the determinate symbiotic organ of *L. japonicus* might indicate that *LjNBCL1* play a role during the symbiotic process.

In *M. truncatula* indeterminate nodules, the RAM marker genes *MtPLETHORA1* and *MtPLETHORA2* (*MtPLT1*/*MtPLT2*) were described as mostly expressed in NVM while *MtPLETHORA3* and *MtPLETHORA4* (*MtPLT3*/*MtPLT4*) were described as mostly expressed in NCM (Roux *et al*., 2014; Franssen *et al*., 2015). We identified *LjPLETHORA1-LIKE* (*LjPLT1-LIKE,* Lj3g3v3245260), *LjPLETHORA2-LIKE* (*LjPLT2-LIKE*, Lj3g3v1778650), *LjPLETHORA3-LIKE* (*LjPLT3-LIKE*, Lj4g3v0708640), *LjPLETHORA4-LIKE* (*LjPLT4-LIKE*, Lj1g3v2841300) genes as the closest homologs of *MtPLETHORA1* to *4* genes in *L. japonicus* and named them according to the literature (Franssen *et al.* 2015). Among these *LjPLTs*, *LjPLT2-LIKE* and *LjPLT4-LIKE* presented characteristic and common expression profiles. They were strongly expressed in the RAM, poorly expressed in primary root, induced during nodule primordia formation and nodule development, and their expressions were drastically reduced from 12 to 20 dpi in nodules. *LjPLT1-LIKE* showed a similar but lower expression profile while *LjPLT3-LIKE* was more expressed in roots than in nodules (Figure S2).

Interestingly, during nodule development, *LjNBCL1, LjPLT2-LIKE* and *LjPLT4-LIKE* showed similar expression profiles. Their transcripts accumulate in nodule primordia and reach a maximum in nodules at 8 dpi (Figure S2). By analogy to *M. truncatula*, *LjPLT2-LIKE* and *LjPLT4-LIKE* could represent marker genes for NVM and NCM activities respectively. Their expression profiles are in agreement with the determinate nature of *L. japonicus* nodules in which NCM activity is transient and also support well the determinate fate of the NVM previously suggested for determinate nodules (Corby, 1988).

LjNBCL1 is required for determinate nodule identity maintenance in *L. japonicus*

NBCL genes encode highly conserved co-transcriptional factors required for several plant developmental processes and especially for plant boundary patterning (Reviewed in Zadnikova and Simon, 2014; Hepworth and Pautot, 2015; Wang *et al*., 2016). The *LjNBCL1* gene belongs to the *NBCL* clade and more precisely to the legume-specific *NBCL1* sub-clade (Couzigou *et al*., 2012; Couzigou *et al*., 2016). *LjNBCL1* was previously described for its role in aerial organ abscission (Couzigou *et al*., 2016).

In the present study, a second *Ljnbcl1 LOTUS RETROELEMENT1* (*LORE1*) mutant line (line 30119830, Figure 2a) was isolated. Self-fertilized heterozygous progeny of this line showed that the *Ljnbcl1* mutation segregated as a monogenic recessive trait with seven homozygous wild-type plants, sixteen heterozygous plants and four plants homozygous for the mutant *Ljnbcl1* locus (X^2: 1,571; df: 2, *p*value: 0,05). The *Ljnbcl1* lines 30119830 (this study) and 30053558 (Couzigou *et al*., 2016, Figure 2a) have similar non-abscission and severe sterility phenotypes, suggesting they are allelic.

In the present work, we studied the two *Ljnbcl1:LORE1* insertion mutants (lines 30119830 and 30053558; Figure 2a) and performed *RNA* interference (*RNAi*) approaches targeting *LjNBCL1* transcripts *(Ljnbcl1:RNAi*; Figure 2a) via hairy-root transformation (Kumagai and Kouchi, 2003; Okamoto *et al*., 2013). The impact of *Ljnbcl1:LORE1* insertion (line 30053558) and *Ljnbcl1:RNAi* on *LjNBCL1* transcript accumulation was assessed by qRT-PCR in 35 dpi nodules. *LjNBCL1* transcript accumulations were drastically reduced by 82 % and reduced by 56 % in *Ljnbcl1:LORE1* mutant nodules (line 30053558) and in *Ljnbcl1:RNAi* transgenic root nodules respectively (Figure 2b,c).

Nodulation experiments using *Ljnbcl1:LORE1* mutant lines (30053558 and 30119830) and *Ljnbcl1:RNAi* hairy-root transformed plants inoculated with *M. loti* revealed a discrete nodule to root conversion phenotype relative to *Mtnoot1* and *Pscoch1* mutants which show about 50 % and 80 % of converted nodules respectively. Wild-type *L. japonicus* GIFU and control *RNAi* transformed plants targeting *β-GLUCURONIDASE* transcripts (*GUS:RNAi*) showed nodules with 100 % wild-type nodule phenotype (Figure 3a,c,e). The *L. japonicus* nodule to root conversion events resulting from *Ljnbcl1* inactivation have a low penetrance in both the *Ljnbcl1:LORE1* lines and the *Ljnbcl1:RNAi* transgenic roots, with only 4 % and 5 % of the nodules that exhibited ectopic root development, respectively (Figure 3b,d,e).

Wild-type *L. japonicus* and *GUS:RNAi* lines showed pink nodules, indicating an efficient nitrogen fixation, however converted nodules from *Ljnbcl1:LORE1* and *Ljnbcl1:RNAi* lines tend to be less pink and more white, indicating an ineffective nitrogen fixation probably due to the nodule to root homeosis (Figure 3 a,b,c,d). As described for the *M. truncatula* and *P. sativum nbcl1* mutants (Ferguson and Reid, 2005; Couzigou *et al*., 2012), *Ljnbcl1:LORE1* and *Ljnbcl1:RNAi* mutant nodule populations have a wild type level of nitrogen fixation (Figure S3) when assessed at the plant level using acetylene reduction

assay (ARA; Koch and Evans 1966). In *Ljnbcl1:LORE1* and *Ljnbcl1:RNAi* lines, the reduced nitrogen fixation of converted nodules might be compensated by the majority of unconverted functional nodules present on each plant.

Ectopic roots arising from the *L. japonicus* determinate nodule originate from the nodule vasculature meristems

Detailed histological analysis of the *GUS:RNAi* transformed root nodules shows the classic wild-type globular shape of determinate nodules (Figure 4a,d; Corby, 1988; Walsh *et al*., 1989; Guinel, 2009). In contrast, in *Ljnbcl1:RNAi* and *Ljnbcl1:LORE1* mutant nodules, an apical nodule-root structure is clearly present on 5% and 4% of nodules respectively (Figure 4b,c). Longitudinal sections of the *Ljnbcl1* nodules reveal the vascular bundle continuum between nodule vascular bundles (NVB) and nodule ectopic root vasculatures. This demonstrates that determinate nodule ectopic roots originate from the NVM as do ectopic roots in indeterminate nodules of *nbcl1* mutants (Figure 4b,c; Ferguson and Reid, 2005; Couzigou *et al*., 2012).

In agreement with the literature describing wild-type determinate nodule organization, transverse sections of the *GUS:RNAi* nodules show peripheral vascular bundles deeply embedded in nodule parenchyma close to the rhizobia infected cells. In determinate nodules, two to three cell layers separate the NVB from the first infected cells (Brown *et al*., 1995; Guinel, 2009; Figure 4d,g; Figure S4). In contrast, in *Ljnbcl1* converted nodules, NVB are surrounded by additional root cortex-like cell layers and tend to be isolated from the nodule infected zone (Figure 4e,f,h,i). In *Ljnbcl1* converted nodules the number of cells separating NVB from infected cells is significantly increased and reaches five to six cortex cell layers (Figure 4e,f; Figure S4). Comparison of completely dissociated *Ljnbcl1* nodule root structures and *L. japonicus* wild-type roots revealed that the number of cortex cell layers surrounding the vasculature (four to five cortex cell layers; Wopereis *et al*., 2000) were not significantly different highlighting the NVB to root identity shift (Figure S5).

In indeterminate and determinate nodules, bundles containing xylem and phloem tissues are surrounded by pericycle cell layers and by an external vascular endodermis cell layer. Previous studies of legume nodule bundle organization have described a collateral organization of xylem and phloem tissues in which phloem tissues face the infected cells and xylem tissues face toward the exterior of the nodule (Pate, 1969; Guinel, 2009). Intriguingly,

in *L. japonicus*, it is the opposite. Bundle organization remains collateral but phloem tissues face toward the exterior of the nodule and the xylem tissues face toward the infection zone (Figure 4g). In *Ljnbcl1* mutant nodules, this atypical organization is conserved but once the NVB that will generate ectopic root starts to dissociate from the infected cells tissues, the xylem and phloem poles delocalize progressively until xylem and phloem poles finally align periclinally and anticlinally to the nodule periphery respectively (Figure 4h,i). This loss of NVB collateral organization in *Ljnbcl1* represents a NVB to root vascular bundle identity shift.

LjNBCL1 is required for nectary development, leaf patterning and for the control of the number of axillary meristem

Database and *L. japonicus* genome analysis reveal that only one *NBCL* gene is present in this plant in contrast to other legume plants. *LjNBCL1* gene expression analysis in the aerial part of wild-type *L. japonicus* shows that *LjNBCL1* transcripts accumulate at low levels in leaves, internodes and in young pods. They were more abundant in nodes and highly abundant in flower from stage 10 to 13 according to the floral stages described in Weng *et al*., 2011 (Figure 5a). These results are in agreement with *LjNBCL1* expression data available from the *Lotus japonicus* Gene Expression Atlas (https://ljgea.noble.org/v2/; Figure S1).

In *Ljnbcl1:LORE1* homozygous mutants, 13 % of the leaves had an additional leaflet relative to *L. japonicus* GIFU suggesting that *LjNBCL1* contributes to leaf patterning by limiting the meristematic potential of the compound leaf (Figure 5b,c,d). In addition, while *L. japonicus* wild-type plants produce one axillary at each leaf axil, *Ljnbcl1:LORE1* homozygous mutants often produced multiple axillaries at a single leaf axil suggesting that *LjNBCL1* is required to control the number and the growth of these axillary meristems (Figure 5e,f).

Together with *Tetragonolobus* and *Bonjeania, Lotus* leaves possess a pair of nectary glands at the base of the petiole, adjacent to the leaf axil, at each node. These nectary glands were proposed to be modified stipules (Figure 5g,i; Irmisch, 1861; Heyn, 1976). Nectary glands are completely absent in *Ljnbcl1* mutants and scanning electron microscopy (SEM) analysis showed no trace of nectary gland development at the leaf axil (Figure 5h,j). As well as loss of nectary glands, *Ljnbcl1* mutants exhibited a significant increase in petiole length relative to the wild-type (Figure 5i,j; Figure S6). These results support a general role for the

NBCL genes in both stipule and nectary gland development by defining the identity of the leaf proximal region, as proposed before in *A. thaliana, M. truncatula* and *P. sativum* (Gourlay *et al*., 2000; Yaxley *et al*., 2001; Ha *et al*., 2003; Hepworth *et al*., 2005; Norberg *et al*., 2005; McKim *et al*., 2008; Couzigou *et al.*, 2012), but in *L. japonicus*, the *LjNBCL1* gene is specifically required for nectary gland formation.

LjNBCL1 gene function is required for floral meristem fate acquisition

The first striking phenotype observed in *Ljnbcl1:LORE1* mutants was their defective flower development leading to almost complete sterility (Figure 6a,b). A *L. japonicus* inflorescence presents one to three adaxial bracts and abaxial nectary glands arising at the pedicel base. This pedicel supports the receptacle from which 21 floral organs develop: five fused sepals, five petals (one adaxial standard, two lateral wings and two abaxial fused keels), ten (nine fused and one unfused) anthers and one carpel (Figure 6c,e,g; Zhang *et al*., 2003; Dong *et al.*, 2005).

Similarly to the *Ljnbcl1* leaves which showed an increased complexity, *Ljnbcl1* mutant inflorescences often display one additional adaxial bract relative to the maximum of three bracts present in wild-type plants (Figure 6g,h). In addition, *Ljnbcl1* mutants are severely impaired in the formation of the floral organs and develop a range of more or less complex structures instead of a normal flower (see below). One characteristic structure formed instead of a flower is the fused trumpet-like lamina structure (Figure 6c,d). In *Ljnbcl1,* the inflorescence nectaries located in abaxial position at the pedicel axil are also absent (Figure 6e,f). In addition, we observed the derepression of an abaxial subtending leaf-like structure outgrowth later called cryptic bract (Figure 6c,d,e,f). Taking into account only the bracts and the cryptic bract, the simplest organ combination that we observed in *Ljnbcl1* was 1 bract and 1 cryptic bract and the most complex structure consisted of 4 bracts and 2 cryptic bracts (Figure 6h). All intermediary combinations exist in the mutant flowers, meaning that only based on bract/cryptic bract, at least 8 organ combinations exist in *Ljnbcl1*.

In addition to the instability of bract/cryptic bract organization, in *Ljnbcl1,* structures formed instead of flowers can take several forms. These were grouped and quantified into the following seven flower-like structures: absence of any structure (Figure 7a, 24 %), prematurely aborted fused trumpet-like lamina structure (Figure 7b, 6 %), developed fused trumpet-like lamina structure (Figure 7c, 11 %), leaf-like structure (Figure 7d, 38 %), more

complex leaf-like structure showing organ separations (Figure 7e, 11%), early aborted floral-like structure (Figure 7f, 7 %) and fully-developed but sterile flower (Figure 7g, 3 %). Taking all inflorescence organs into account, *Ljnbcl1* mutants presented at least 56 different combinations of inflorescence organization. These flower phenotypes highlight the crucial role of the *LjNBCL1* gene for the acquisition and the determination of floral meristem identity.

Secondary inflorescence meristem and floral primordia development are affected in the *Ljnbcl1* mutant

In *L. japonicus*, as in other legumes, at the floral transition, the apical meristem of each shoot becomes a primary inflorescence meristem (I1) which produces a secondary inflorescence meristem (I2) at each node, in the axil of the leaf, and it is the I2 that generates the floral meristems (Benlloch *et al*., 2015). When *L. japonicus* floral meristems partition from the I2, the differentiated I2 becomes covered by trichomes (Feng *et al.*, 2006). To understand the defects in floral development of *Ljnbcl1* mutants, we studied the ontogeny of the inflorescence of *Ljnbcl1:LORE1* mutant plants by SEM.

SEM analysis showed that the I1 inflorescence of wild-type *L. japonicus* formed an I2 in the axil of the compound leaf. Floral meristems derived from the I2 of the previous node were seen, adjacent to trichomes which covered the fully differentiated I2 (Figure 8a,b,c).

In contrast, the structures observed in the inflorescence apex of the *Ljnbcl1:LORE1* mutants were very different. At very early stages of their development, the leaf primordia subtended at their axils a poorly developed dome that was separated from the I1 by a line of developing trichomes similar to the ones observed in the wild-type I2 at stage five when they differentiate after partition of the floral meristems (Feng *et al*., 2006). Structures looking-like wild-type I2 of previous developmental stages were never detected in the mutant apex. The small domes delimited by the trichomes that should correspond to floral meristems did not progress along with the development of the leaf primordia (Figure 8d,e,f). These atypical structures found in the *Ljnbcl1:LORE1* inflorescence apex suggest that *Ljnbcl1* I2 develop abnormally producing aberrant floral meristem-like structures that do not progress normally. This analysis shows that the defects in reproductive structures start very early in *Ljnbcl1:LORE1* inflorescence ontogeny.

DISCUSSION

The numerous vegetative and reproductive developmental defects observed in *Ljnbcl1* mutants and the absence of an *LjNBCL2* sequence in databases suggest that there is only one *NBCL (LjNBCL1)* in the genome of *L. japonicus* ecotype GIFU in contrast to other legume plants studied, which have at least two distinct *NBCL* genes. In this work, we show that in the determinate nodules of *L. japonicus*, *LjNBCL1* gene is constitutively expressed in roots, induced during nodulation and thus behaves as the *MtNOOT1* gene (Couzigou *et al.*, 2012). We demonstrate that, despite the differences existing in determinate nodule organogenesis and organization, *LjNBCL1* gene function in maintenance of nodule identity through NVB root identity repression is conserved. A similar nodule to root conversion phenotype was described in *Glycine max* determinate nodules inoculated with *Bradyrhizobium japonicum* mutant strains (ΔphyR, ΔecfG; Gourion *et al.*, 2009) but the origin of the nodule ectopic roots was not described in this context. In this study we demonstrate that ectopic roots arising from determinate nodules are initiated from the NVB as hypothesized by Couzigou and Ratet (2015). This finding is in agreement with the literature describing nodule ectopic roots that initiate from NVM (VandenBosch *et al.*, 1985; Akasaka *et al.*, 1998; Voroshilova *et al.,* 2003; Ferraioli *et al.*, 2004; Ferguson and Reid, 2005; Sinharoy and DasGupta, 2009; Couzigou *et al.*, 2012; Couzigou and Ratet, 2015). The low penetrance of the nodule to root conversion in *Ljnbcl1* compared to *Pscoch1* or *Mtnoot1* suggests that one of the roles of the NCM in indeterminate nodules is to maintain active NVM to confer indeterminate growth. In determinate nodules, there is no persistent NCM: once vascular strand anastomosis has occurred at the nodule apex, the NVM becomes determinate leading to NVB growth arrest (Corby, 1988; Guinel, 2009). We suggest that this determinate NVM status makes determinate nodule less susceptible to root conversion because homeosis requires constitutively active NVM. Moreover, we also report that the *L. japonicus* NVB harbours a non-canonical xylem/phloem collateral organization with xylem and phloem facing toward the infected cell and the exterior of the nodule, respectively. We revealed also that this xylem/phloem collateral organization is lost in converted nodules suggesting that *Ljnbcl1* NVB identity is lost and root identity is acquired during homeosis.

NBCL genes functions are required for lateral organ determinacy, leaf proximal/distal patterning and for the control of shoot branching, and these functions are conserved across dicots and grasses (Ha *et al.*, 2003; Hepworth *et al.*, 2005; Norberg *et al.*, 2005; Couzigou *et al.*, 2012; Tavakol *et al.,* 2015). The present study shows that in *L. japonicus,* the *NBCL1*

gene fulfils the same functions. The six leaflets phenotype and the additional axillaries observed in *Ljnbcl1* reflect a reduction of the determinacy of lateral organs. Also, at the base of leaves, *NBCL* genes repress cell division and promote lateral organ differentiation. In *Ljnbcl1,* the petiole length increase and the lack of nectary glands may reflect the failure of these two processes. Wild-type *L. japonicus* exhibits a pair of nectary glands that have been for a long time proposed to be ontologically related to stipules (Irmisch, 1861; Heyn, 1976). The complete absence of nectary glands in *Ljnbcl1* mutants definitively supports an ontological relationship between stipules and nectary glands. *LjNBCL1* is thus essential for nectary gland initiation and development in accordance with the role of NBCL as a master regulator of stipule initiation, development and determinacy in *P. sativum*, *M. truncatula* and in *A. thaliana* (Gourlay *et al.* 2000; Yaxley *et al.,* 2001; McKim *et al.*, 2008; Couzigou *et al.*, 2012).

In *A. thaliana*, *P. sativum* or *M. truncatula, NBCL* loss-of-functions modify the number of floral organs, the symmetry of the flower and impact the identity of floral organs (Yaxley *et al.*, 2001; Ha *et al.*, 2003, 2004; Hepworth *et al.*, 2005; Norberg *et al.*, 2005; Xu *et al.*, 2010; Couzigou *et al.*, 2012). The *L. japonicus nbcl1* mutant showed severe defects in floral initiation and patterning characterized by a large range of floral phenotypes, ranging from wild-type-like flowers to complete absence of floral organs, suggesting a high instability in cell differentiation/proliferation processes in the floral primordia. The floral meristem determinacy acquisition is often associated with the suppression of the subtending bract. Indeed, mutants affected in floral meristem fate acquisition present floral meristem mis-establishment and enlargement of a cryptic bract (Schultz and Haughn, 1991; Levin and Meyerowitz, 1995; Long and Barton, 2000; Hepworth *et al.*, 2005; Norberg *et al.*, 2005; Hepworth *et al.*, 2006; Karim *et al.*, 2009). In *Ljnbcl1,* a floral cryptic bract develops indicating that the floral meristem is not fully determinate. The floral bract outgrowth and the strong flowering defects observed in *Ljnbcl1* mutants indicate that *Lj*NBCL1 functions are conserved for floral meristem determinacy in *L. japonicus* and suggests that *Lj*NBCL1 is essential to allow the expression of floral meristem identity genes. In *A. thaliana*, *At*BOP1/2 contribute to floral initiation and patterning by promoting the expression of *LEAFY* (*LFY*) and *APETALA1* (*AP1*), the main *A. thaliana* floral meristem identity genes (Norberg *et al.*, 2005; Blázquez *et al.*, 2006; Karim *et al.*, 2009; Xu et *al.*, 2010). Therefore, future experiments will indicate if the severe floral defects of the *Ljnbcl1* mutants are related to reduced expression of the *L. japonicus LFY* and *AP1* orthologs.

The fused trumpet-like lamina structure in place of flowers is a distinctive *Ljnbcl1* mutant phenotype that is reminiscent of the *A. thaliana Atcup-shaped cotyledon1/2/3* (*Atcuc1/2/3*) double and triple mutants, which present fusions of different organs such as cotyledons, sepals, stamens, leaves, stems and pedicels (Aida *et al*., 1997; Takada *et al*., 2001; Hibara *et al*., 2006). *CUC* genes are, like *NBCL* genes, involved in organ separation processes and in the establishment of boundary zones, where they are consistently expressed and function to repress growth (Wang *et al*., 2016). In *Arabidopsis*, *At*CUC1 promotes the expression of the *AtLIGHT-DEPENDENT SHORT HYPOCOTYLS 3 (AtLSH3)* and its paralog *AtLSH4,* which are members of the *Arabidopsis LSH1* and *Oryza G1* genes family (*ALOG;* Cho and Zambryski, 2011; Takeda *et al.,* 2011). Furthermore, in *Lycopersicon esculentum* it has been shown that ALOG proteins are able to interact with NBCL proteins (Xu *et al*., 2016). Thus, in *L. japonicus,* boundary zone patterning and regulation might be carried-out through a similar *CUC/ALOG/NBCL* module in which *LjNBCL1* plays a major role.

In *L. japonicus*, floral meristems derive from partitioning of the I2 secondary inflorescence meristem (Feng *et al.*, 2006). In the *Ljnbcl1* inflorescence apex, early in its development, the only trace of I2-like structure observed is a line of developing trichomes, identical to those observed in wild-type differentiating I2 at stage five after floral primordia formation (Feng *et al.*, 2006). This line delimited a small dome corresponding to an abnormal floral primordium. The absence of structures looking-like wild-type I2 at earlier developmental stages in *Ljnbcl1* apex suggests that the development of these mutant I2s are very premature and fast. This probably negatively affects floral meristem initiation and fits well with the severe floral development defects of the *Ljnbcl1* mutants. Acquisition of I2 meristem identity in pea is known to be controlled by *VEGETATIVE1* (*VEG1*), a MADS-box gene from the same clade as *AP1* (Berbel *et al*., 2012). It is likely that *VEG1* function is conserved in other legumes, including *L. japonicus*, where *VEG1* orthologs are present (Benlloch *et al.*, 2015). In agreement with this, the phenotype of the soybean *dt2* mutant, with a dominant mutation in the ortholog of *VEG1* agrees with the conservation of the VEG1 function (Ping *et al*., 2014). In the same way that the *At*BOP1/2 promote the expression of the floral meristem identity genes *LFY* and *AP1* (Karim *et al*., 2009; Xu *et al.,* 2010), *Lj*NBCL1 might also be required for the proper expression of the *L. japonicus VEG1* ortholog.

MATERIALS AND METHODS

Plant material and growth conditions. *L. japonicus* ecotype GIFU (Handberg and Stougaard, 1992) and the corresponding *Ljnbcl1 LORE1* insertional mutant lines (line 30053558, Couzigou *et al*., 2016 and line 30119830, this study) obtained from the *LORE1* insertion mutant collection (https://lotus.au.dk; Mun *et al*., 2016; Malolepszy *et al*., 2016) were used. *L. japonicus* seeds were scarified using sand paper, surface-sterilized 30 min with sodium hypochlorite, washed three times with sterile water and left overnight in sterile water under agitation at 4 °C. Seeds were germinated on agar plates (Kalys Biotech, HP696-5, 7 g l^{-1}) for 2 days at 24°C. For *in vitro* nodulation studies, *L. japonicus* seedling were grown on Buffered Nodulation Media (Ehrhardt *et al*., 1992), solidified with Kalys agar 7 g l^{-1} and supplemented with 0,5 μM of 2-aminoethoxyvinyl glycine (Sigma-aldrich). For studies of nodulation in pots, a sand/perlite mixture was used (1/2, v/v). For vegetative development and flowering studies, a loam/peat/sand mixture was used (70/3,5/7, v/v/v; http://www.puteaux-sa.fr) with expensed clay pebbles at the bottom of the pot. *L. japonicus* were grown under a 16/8 h light-dark cycle, a 23/23 °C day-night temperature regime, 60 % relative humidity and 200 μE light intensity. Plants were watered three times a week, twice with water, once with nutritive solution, alternately. For nodulation studies a N-free nutritive solution (Plant prod, NPK 0-15-40) was used, otherwise, a N+ nutritive solution (Soluplant, NPK16 6 26) was used.

Rhizobial strain, growth conditions and inoculation. *M. loti* wild-type strain NZP-2235 (Jarvis *et al.* 1982) was used for *L. japonicus* nodulation. Rhizobia were grown on solid or liquid YEB (Krall *et al*., 2002) for 2 days under darkness at 30 °C. For *in vitro* and sand/perlite nodulation, *L. japonicus* seedling or hairy-root transformed plant were inoculated with 1 ml and 25 ml of *M. loti* suspension at OD: 0.1, respectively.

***L. japonicus* DNA extraction.** *L. japonicus* DNA was extracted from young leaves using a phenol/chloroform procedure. DNA was precipitated using cold sodium acetate 3 M; isopropanol (0.1:1) and washed using ethanol 70 %. DNA samples were dried and resuspended in sterile water. An RNase treatment was finally performed (Roche).

Ljnbcl1:LORE1 **insertional mutant genotyping strategy.** In line 30053558, the *LORE1* retro-element is inserted 2077 bp after the ATG codon on genomic DNA sequence, 1134 bp after the AUG codon on mRNA sequence (NCBI Acc. No.: JN408495), between amino acids isoleucine 378 and glutamic acid 379 of the *Lj*NBCL1 protein (NCBI Acc. No.: AEM62768). In line 30119830, the *LORE1* retro-element is inserted 1803 bp after the ATG codon on genomic DNA sequence, 860 bp after the AUG codon on mRNA sequence and between amino acids leucine 286 and alanine 287 of the *Lj*NBCL1 protein. The presence of the 5406 bp length *LORE1* TY3-gypsy type retrotransposon (NCBI Acc. No.: AJ966990) at the *LjNBCL1* locus was checked by PCR in lines 30053558 and 30119830 using primers described in the Table S1.

RNA interference. The 263 bp *RNAi_LjNBCL1#1* amplicon was designed against the *LjNBCL1* mRNA sequence from nucleotide 474 to nucleotide 736. Amplicon specificity was determined through BLAST analysis (https://blast.ncbi.nlm.nih.gov/Blast.cgi?PROGRAM=blastn) against the *L. japonicus* genome. *RNAi_LjNBCL1#1* amplicons were amplified from *L. japonicus* ecotype GIFU cDNA using Phusion® High-Fidelity DNA Polymerase (NEB) following the manufacturer's recommendation, cloned in pENTR/D-TOPO vector (Life technologies) and introduced by Gateway LR recombination (Invitrogen) in both anti-sense and sense in a pFRN-RNAi binary vector (Gonzalez-Rizzo *et al*., 2006; derived from binary pFGC5941 vector; NCBI Acc. No.: AY310901). Constructs of interest were introduced into *Agrobacterium rhizogenese (A. rhizogenese)* ARqua1 (streptomycin[R]-derivative strain of A4T; *Quandt et al*., 1993) by electroporation (Bio-rad, *E. coli* Pulser). The *LjNBCL1:RNAi* construction transcript structure was predicted using the online software RNAfold and the « minimum free energy » pairing algorithm (rna.tbi.univie.ac.at/cgi-bin/RNAfold.cgi). An ARqua1 strain expressing an *RNAi* construct designed against the *β-GLUCURONIDASE* transcripts (*GUS*:*RNAi,* Gonzalez-rizzo *et al*., 2006) was used as control. Primers used for the RNA interference strategy are described in Table S2.

A. rhizogenes* mediated *L. japonicus* hairy-root transformation. *L. japonicus* hairy-root transformations were performed as described in Kumagai and Kouchi 2003 and Okamoto *et al*., 2013 with minor modifications using the *A. rhizogenes* ARqua1 strain. Hairy-roots were subsequently inoculated with *M. loti* and nodules were observed at 35 dpi.

qRT-PCR Gene expression analyses. Total RNA extractions were performed from frozen tissues using TRIzol® reagent (Ambion) following manufacturer's recommendations for underground organs and using a sodium borate / TRIzol procedure (adapted from Høgslund *et al.,* 2009) for aboveground organs. RNA samples were treated with the TURBO DNA-free™ Kit (Ambion) according to the manufacturer's recommendations. Full-length cDNA were synthesized using SuperScript™ II Reverse Transcriptase kit (Invitrogen) in the presence of Ribolock RNase Inhibitor (Thermoscientific). qRT-PCR reactions were performed using the LightCycler FastStart DNA Master SYBR Green I kit on a Light Cycler 480 II device according to manufacturer's instructions (Roche). Cycling conditions were as follows: 1 pre-incubation cycle (95 °C, 10 min), 40 amplification cycles [(denaturation: 95 °C, 10 s), (hybridization: 60 °C, 15 s), (elongation: 72 °C, 15 s)], 1 melting curve cycle [(denaturation: 95 °C, 15 s), (hybridization: 55 °C, 1 min), (denaturation: 95 °C)], 1 cooling cycle (40 °C, 30 s). Cycle threshold and primer specificity analysis were performed using the LightCycler 480 software release 1.5.0 SP4. Primer efficiencies were calculated with LinReg PCR: Analysis of Real-Time PCR Data, version 11.1. *LjPP2A* and *LjUBC* were used as reference genes for gene expression normalization. Primers used for qRT-PCR are provided in Table S3.

Light Microscopy and sample preparation. Sample sections embedded in technovit resine were treated essentially as described in Van de Velde *et al*. (2006). Fixed samples were infiltrated 15 min under vacuum (≈500 mm Hg) in sodium cacodylate buffer pH: 7 (0.05 M), glutaraldehyde 1 % and formaldehyde 4 % and incubated at 4 °C overnight. After dehydration in successive ethanol bathes, samples underwent successive 1 h ethanol/technovit stock solution bathes (3:1, v/v), (1:1, v/v), (1:3, v/v) and three (1:0, v/v) at 4 °C under agitation. Samples were embedded in technovit resin using teflon Histoform S

embedding moulds (Heraeus Kulzer). 5 μm sections were cut using a microtome (Leica, RM 2155) and tungsten disposable blade (Leica, TC-65). Sections were stained for 10 min with toluidine blue (0.02 %), observed with a microscope (Olympus, BX53) and digital images were acquired using cellSens Standard software (Olympus life science).

Acetylene reduction assay. Acetylene reduction assays (ARA) were performed on individual plants inoculated with *M. loti* at 35 dpi with a protocol modified from Koch and Evans (1966). Basically, the nodulated root system of one plant was placed in 21 ml glass vial sealed with rubber septa in presence of 200 μl of water. Acetylene gas (500 μl) was injected into each vial and 2 h incubation was performed. For each sample, 1 ml of gas was injected. Ethylene production was measured using a Gas Chromatograph (Agilent Technologies, 7820A) equipped with a GS-Alumina column (50 m x 0,53 mm) with hydrogen as carrier gas. Column temperature and gas flow were adjusted at 120 °C and at 7.5 ml min^{-1}, respectively.

Scanning electron microscopy. Nectary glands and inflorescence apex from *Ljnbcl1* homozygous mutants and *LjNBCL1* wild-type siblings were fixed in FAE (ethanol 50 %, formaldehyde 3.7 % and glacial acetic acid 5%) through 5 successive vacuum pulses at ≈ 500 mm Hg for 5 min and incubated in fresh FAE at 4 °C over-night under darkness. Samples were dehydrated with successive 30 min ethanol baths (70 %, 80 %, 100 %, 100 %). Critical point drying was performed at 17 °C and 62 bar (900 psi) for 90 min using liquid CO_2 as the transitional fluid in a critical point chamber (Polaron). Samples were dried by reaching the critical point of CO_2 by adjusting the temperature and pressure to 34 °C and 80 bars (1200 psi), during 30 min. Dried samples were prepared, stuck on a support and sputter-coated with argon-platinium plasma at 6-7 cm distance and 45 mA intensity for 15 sec in a sputtering chamber (Leica microsystems, EM MED020). Scanning electron micrographs were acquired using a FIB SEM AURIGA compact (Zeiss) at E.H.T.: 1-2 kV.

Data availability. The mutant used in this study is freely available from the *LORE1* insertion mutant collection (https://lotus.au.dk).

Author contributions

P.R. and K.M. conceived the project and designed the experiments. K.M. performed the gene expression analysis, the nodule phenotypes characterization, the histology, the optical microscopy, the *Lj*GEA data mining and the acetylene reduction assays. K.M. and J.G. performed the genotyping and analyzed the aerial phenotypes. K.M. and B.B. performed the RNAi approaches. K.M. and A.B-T performed the SEM. K.M., J.G., A.B-T., B.B. F.M. and PR analyzed the data. S-U. A. generated the *L. japonicus LORE1* insertional mutant collection and performed the *LORE1* mutant screen. K. M., P. R. and F.M. wrote the article and K.M., P.R., J. G., A.B-T, F.M. and S-U. A. carefully revised the article.

SHORT SUPPORTING INFORMATION LEGENDS

The following Supporting Information are available for this article:

Figure S1. *LjNBCL1* gene expression profile using the *Lotus japonicus* Gene Expression Atlas.

Figure S2. *Lotus japonicus PLETHORA1-4* genes expression kinetics during nodulation.

Figure S3. *Ljnbcl1* mutation does not affect symbiotic nitrogen fixation.

Figure S4. Number of cells separating nodule vascular bundle from infected cells is increased in *Ljnbcl1* mutants.

Figure S5. Number of cortex cell layers present in *Ljnbcl1* nodule ectopic root is similar to *L. japonicus* root.

Figure S6. *Ljnbcl1* petiole length is increased.

Table S1. Oligonucleotides used for *LORE1* insertions genotyping.

Table S2. Oligonucleotides used for the *LjNBCL1:RNAi* strategy.

Table S3. Oligonucleotides used for qRT-PCR analysis.

REFERENCES

Aida, M., Ishida, T., Fukaki, H., Fujisawa, H. and Tasaka, M. (1997) Genes involved in organ separation in *Arabidopsis*: An analysis of the *cup-shaped cotyledon* mutant. *Plant Cell*, Vol. 9, pp. 841–857. DOI: https://doi.org/10.1105/tpc.9.6.841.

Aida, M. and Tasaka, M. (2006a) Genetic control of shoot organ boundaries. *Curr. Opin. Plant Biol.*, Vol. 9, pp. 72–77. DOI 10.1016/j.pbi.2005.11.011.

Aida, M. and Tasaka, M. (2006b) Morphogenesis and patterning at the organ boundaries in the higher plant shoot apex. *Plant Mol. Biol.*, Vol. 60, pp. 915–928. DOI 10.1007/s11103-005-2760-7.

Akasaka, Y., Mii, M. and Daimon, H. (1998) Morphological alterations and root nodule formation in *Agrobacterium rhizogenes*-mediated transgenic hairy roots of Peanut (*Arachis hypogaea L.*). *Ann. Bot.*, Vol. 81, pp. 355–362.

Benlloch, R., Berbel, A., Ali, L., Gohari, G., Millan, T. and Madueño, F. (2015) Genetic control of inflorescence architecture in legumes. *Frontiers in Plant Science*, Vol. 6, pp. 543. doi: 10.3389/fpls.2015.00543.

Berbel, A., Ferrándiz, C., Hecht, V., Dalmais, M., Lund, O.S., Sussmilch, F. C., *et al.* (2012). *VEGETATIVE1* is essential for development of the compound inflorescence in pea. *Nature Communications*, 3, 797.

Blázquez, M.A., Ferrándiz, C., Madueño, F. and Parcy, F. (2006) How floral meristems are built. *Plant Molecular Biology*, Vol. 60(6), pp. 855–870.

Brown, S.M., Oparka, K.J., Sprent, J.I. and Walsh, K.B. (1995) Symplastic transport in soybean root nodules. *Soil Biol. Biochem.*, Vol. 27(4–5) pp. 387–399. doi:10.1016/0038-0717(95)98609-R.

Chen, Y., Chen, W., Li, X., Jiang, H., Wu, P., Xia, K., Yang, Y. and Wu, G. (2013) Knockdown of *LjIPT3* influences nodule development in *Lotus japonicus*. *Plant Cell Physiol.*, Vol. 55(1), pp. 183-193. doi:10.1093/pcp/pct171.

Cho, E. and Zambryski, P.C. (2011) *ORGAN BOUNDARY1* defines a gene expressed at the junction between the shoot apical meristem and lateral organs. *Proceedings of the National Academy of Sciences, USA* Vol.108, pp. 2154–2159. doi: 10.1073/pnas.1018542108.

Corby, H.D.L. (1988) Types of rhizobial nodules and their distribution among the Leguminosae. *Kirkia*, Vol.13(1), pp. 53–124.

Couzigou, J.M., Magne, K., Mondy, S., Cosson, V., Clements, J. and Ratet P. (2016) The legume *NOOT-BOP-COCH-LIKE* genes are conserved regulators of abscission, a major agronomical trait in cultivated crops. *New Phytologist*, Vol. 209, pp. 228–240. DOI: 10.1111/nph.13634.

Couzigou J.M. and Ratet P. (2015) *NOOT*-dependent control of nodule identity: nodule homeosis and meristem perturbation. Biological Nitrogen Fixation, Volume 1, First Edition. Edited by Frans J. de Bruijn. DOI:10.1002/9781119053095.ch49

Couzigou, J.M., Zhukov, V., Mondy, S., Abu el Heba, G., Cosson, V., Ellis, T.H., Ambrose, M., Wen, J., Tadege, M., Tikhonovich, I., Mysore, K.S., Putterill, J., Hofer, J., Borisov, A.Y. and Ratet P. (2012) *NODULE ROOT* and *COCHLEATA* maintain nodule development and are legume orthologs of *Arabidopsis BLADE-ON-PETIOLE* genes. *Plant Cell*, Vol. 24, pp. 4498-510; PMID:23136374. http://dx.doi.org/10.1105/ tpc.112.103747.

Czechowski, T., Stitt, M., Altmann, T., Udvardi, M.K. and Scheible, W.R. (2005) Genome-wide identification and testing of superior reference genes for transcript normalization in *Arabidopsis*. *Plant Physiol.*, Vol. 139, pp. 5–17. PMCID: PMC1203353. DOI: 10.1104/pp.105.063743.

Dong, Z.C., Zhao, Z., Liu, C.W., Luo, J.H., Yang, J., Huang, W.H., Hu, X.E., Wang, T.L. and Luo, D. (2005) Floral Patterning in *Lotus japonicus*. *Plant Physiol.*, Vol. 137, pp. 1272–1282. doi/10.1104/pp.104.054288.

Ehrhardt, D.W., Atkinson, E.M. and Long, S.R. (1992) Depolarization of alfalfa root hair membrane potential by *Rhizobium meliloti* Nod factors. *Science*, Vol. 256, Issue 5059, pp. 998–1000. DOI: 10.1126/science.10744524.

Ferguson, B.J. and Reid, J.B. (2005) *Cochleata*: getting to the root of legume nodules. *Plant Cell Physiol.*, Vol. 46, pp. 1583–1589.

Feng, X., Zhao, Z., Tian, Z., Xu, S., Luo, Y., Cai, Z., Wang, Y., Yang, J., Wang, Z., Weng, L., Chen, J., Zheng, L., Guo, X., Luo, J., Sato, S., Tabata, S., Ma, W., Cao, X., Hu, X., Sun, C. and Luo, D. (2006) Control of petal shape and floral zygomorphy in *Lotus japonicus*. *PNAS,* Vol. 103, no. 13, pp. 4970-4975. Doi/10.1073/pnas.0600681103.

Ferraioli, S., Tatè, R., Rogato, A., Chiurazzi, M. and Patriarca, E. J. (2004) Development of ectopic roots from abortive nodule primordia. *MPMI*, Vol. 17, No. 10, 2004, pp. 1043–1050. http://dx.doi.org/10.1094/MPMI.2004.17.10.1043

Franssen, H.J., Xiao, T.T., Kulikova, O., Wan, X., Bisseling, T., Scheres, B. and Heidstra, R. (2015) Root developmental programs shape the *Medicago truncatula* nodule meristem. *Development*, Vol. 142, pp. 2941-2950. http://doi: 10.1242/dev.120774.

Gonzalez-rizzo, S., Crespi, M. and Frugier, F. (2006) The *Medicago truncatula CRE1* cytokinin receptor regulates lateral root development and early symbiotic interaction with *Sinorhizobium meliloti*. *The Plant Cell*, Vol. 18, pp. 2680–2693. http://doi.org/10.1105/tpc.106.043778.

Gourion, B., Sulser, S., Frunzke, J., Francez-Charlot A., Stiefel, P., Pessi, G., Vorholt, J.A. and Fischer, HM. (2009) The PhyR-sigma(EcfG) signalling cascade is involved in stress response and symbiotic efficiency in *Bradyrhizobium japonicum*. *Mol. Microbiol.*, Vol. 73, pp. 291–305. doi: 10.1111/j.1365-2958.2009.06769.x.

Gourlay, C.W., Hofer, J.M.I. and Ellis, T.H.N. (2000) Pea compound leaf architecture is regulated by interactions among the genes *UNIFOLIATA, COCHLEATA, AFILA* and *TENDRIL-LESS*. *Plant Cell*, Vol. 12, pp., 1279–1294. PMCID: PMC149102.

Guether, M., Balestrini, R., Hannah, M., He, J., Udvardi, M.K. and Bonfante, P. (2009) Genome-wide reprogramming of regulatory networks, transport, cell wall and membrane biogenesis during arbuscular mycorrhizal symbiosis in *Lotus japonicus*. *New Phytologist*, Vol. 182(1), pp. 200-212. doi: 10.1111/j.1469-8137.2008.02725.x.

Guinel, F. C. (2009). Getting around the legume nodule: I. The structure of the peripheral zone in four nodule types. *Botany*, Vol. 87, pp. 1117–1138. http://doi:10.1139/B09-074

Ha, C. M., Jun, J. H., Nam, H. G. and Fletcher, J. C. (2004). *BLADE-ON-PETIOLE1* encodes a BTB/POZ domain protein required for leaf morphogenesis in *Arabidopsis thaliana*. *Plant Cell Physiol.*, Vol. 45(10), pp. 1361–1370. DOI: 10.1093/pcp/pch201.

Ha, C.M., Jun, J.H., Nam, H.G. and Fletcher, J.C. (2007). *BLADE-ON-PETIOLE* 1 and 2 control *Arabidopsis* lateral organ fate through regulation of LOB domain and adaxial-abaxial polarity genes. *Plant Cell*, Vol. 19(6), pp. 1809-25. PMID: 17601823. PMCID: PMC1955725. DOI: 10.1105/tpc.107.051938.

Ha, C.M., Kim, G.T., Kim, B.C., Jun, J.H., Soh, M.S., Ueno, Y., Machida, Y., Tsukaya, H. and Nam, H.G. (2003). The *BLADE-ONPETIOLE 1* gene controls leaf pattern formation through the modulation of meristematic activity in *Arabidopsis*. *Development*, Vol. 130, pp. 161–172. PMID: 12441300.

Handberg, K. and Stougaard, J. (1992) *Lotus japonicus*, an autogamous, diploid legume species for classical and molecular genetics. *Plant Journal*, Vol. 2, pp. 487–496. DOI: 10.1111/j.1365-313X.1992.00487.x.

Hepworth, S.R., Klenz, J.E. and Haughn, G.W. (2006). UFO in the Arabidopsis inflorescence apex is required for floral-meristem identity and bract suppression, *Planta,* 223 769–778.

Hepworth, S. R. and Pautot, V. A. (2015). Beyond the divide : boundaries for patterning and stem cell regulation in plants. *Front. Plant Sci.*, Vol. 6, pp. 1052. http://doi.org/10.3389/fpls.2015.01052

Hepworth, S. R., Zhang, Y., Mckim, S., Li, X. and Haughn, G. W. (2005). *BLADE-ON-PETIOLE* – Dependent Signaling Controls Leaf and Floral Patterning in *Arabidopsis*. *The Plant Cell*, Vol. 17, pp. 1434–1448. http://doi/10.1105/tpc.104.030536.

Heyn, C.C. (1976) An old question revived: "What are the stipules of *Lotus*?" *Lotus Newsletter*, Vol. 7, pp. 3-5.

Hibara, K.I., Rezaul Karim, Md., Takada, S., Taoka, K.I., Furutani, M., Aida, M. and Tasaka, M. (2006) *Arabidopsis CUP-SHAPED COTYLEDON3* regulates postembryonic shoot meristem and organ boundary formation. *The Plant Cell*, Vol. 18, pp. 2946–2957. doi/10.1105/tpc.106.045716.

Høgslund, N., Radutoiu, S., Krusell, L., Voroshilova, V., Hannah, M.A., Goffard, N., Sanchez, D.H., Lippold, F., Ott, T., Sato, S., Tabata, S., Liboriussen, P., Lohmann, G.V., Schauser, L., Weiller, G.F., Udvardi, M.K. and Stougaard, J. (2009) Dissection of

symbiosis and organ development by integrated transcriptome analysis of *Lotus japonicus* mutant and wild-type plants. *PLoS One*, Vol. 4(8):e6556. doi: 10.1371/journal.pone.0006556.

Irmisch, T. (1861) Noch einige Beobachtungen über die Stipulae bei *Lotus*, *Tetragonolobus* und *Bonjeania*. *Bot. Zeitg*, Vol. 19, pp. 329-331.

Jarvis, B. D. W., Pankhurst, C. E. and Patel, J. J. (1982) *Rhizobium loti*, a new species of legume root nodule bacteria. *Int. J. Syst. Bacteriol.*, Vol. 32, pp. 378–380.

Jost, M., Taketa, S., Mascher, M., Himmelbach, A., You, T., Shahinnia, F., Rutten, T., Druka, A., Schmutzer, T., Steuernagel, B., Beier, S., Taudien, S., Scholz, U., Morgante, M., Waugh, R. and Stein, N. (2016) A homolog of BLADE-ON-PETIOLE 1 and 2 (BOP1/2) controls internode length and homeotic changes of the barley inflorescence. *Plant Physiology*, 171(2):1113-27. DOI: 10.1104/pp.16.00124.

Karim, M.R., Hirota, A., Kwiatkowska, D., Tasaka, M. and Aida, M. (2009) A role for *Arabidopsis PUCHI* in floral meristem identity and bract suppression. *The Plant Cell*, Vol. 21(5), pp. 1360–1372.

Khan, M., Xu, M., Murmu, J., Tabb, P., Liu, Y., Storey, K., McKim, S.M., Douglas, C.J. and Hepworth, S.R. (2012). Antagonistic interaction of BLADE-ON-PETIOLE1 and 2 with BREVIPEDICELLUS and PENNYWISE regulates *Arabidopsis* inflorescence architecture. *Plant Physiol.*, Vol. 158, pp. 946–960. PMCID: PMC3271780. DOI: 10.1104/pp.111.188573.

Khan, M., Ragni, L., Tabb, P., Salasini, B.C., Chatfield, S., Datla, R., Lock, J., Kuai, X., Després, C., Proveniers, M., *et al.* (2015). Repression of lateral organ boundary genes by *PENNYWISE* and *POUND-FOOLISH* is essential for meristem maintenance and flowering in *Arabidopsis*. *Plant Physiol.*, Vol. 169, pp. 2166–2186. PMCID: PMC4634066. DOI: 10.1104/pp.15.00915.

Koch, B. and Evans, H. J. (1966) Reduction of acetylene to ethylene by soybean root nodules. *Plant Physiol.*, Vol. 41, pp. 1748-1750. PMCID: PMC550603.

Krall, L., Wiedemann, U., Unsin, G., Weiss, S., Domke, N. and Baron, C. (2002). Detergent extraction identifies different VirB protein subassemblies of the type IV secretion machinery in the membranes of *Agrobacterium tumefaciens*. *PNAS*, vol. 99, no. 17, pp. 11405–11410. http://doi_10.1073_pnas.172390699.

Kumagai, H. and Kouchi, H. (2003) Gene silencing by expression of hairpin RNA in *Lotus japonicus* roots and root nodules. *MPMI*, Vol. 16, No. 8, pp. 663–668. DOI: 10.1094/MPMI.2003.16.8.663.

Levin, J.Z. and Meyerowitz, E.M. (1995). UFO: An Arabidopsis gene involved in both floral meristem and floral organ development. *Plant Cell*, 7, 529 –548.

Long, J. and Barton M.K. (2000). Initiation of axillary and floral meristems in Arabidopsis. *Developmental biology,* 218, 341–353. doi:10.1006/dbio.1999.9572.

Małolepszy, A., Mun, T., Sandal, N., Gupta, V., Dubin, M., Urbański, D., Shah, N., Bachmann, A., Fukai, E., Hirakawa, H., Tabata, S., Nadzieja, M., Markmann, K., Su, J., Umehara, Y., Soyano, T., Miyahara, A., Sato, S., Hayashi, M., Stougaard, J. and Andersen, S.U. (2016) The *LORE1* insertion mutant resource. *Plant Journal*, Vol. 88(2), pp. 306-317. doi: 10.1111/tpj.13243. Epub 2016 Sep 27.

McKim, S.M., Stenvik, G.E., Butenko, M.A., Kristiansen, W., Cho, S.K., Hepworth, S.R., Aalen, R.B. and Haughn, G.W. (2008) The *BLADE-ON-PETIOLE* genes are essential for abscission zone formation in *Arabidopsis*. *Development*, Vol. 135, pp. 1537-1546. DOI:10.1242/dev.012807.

Mun, T., Bachmann, A., Gupta, V., Stougaard, J. and Andersen, S.U. (2016) Lotus Base: An integrated information portal for the model legume *Lotus japonicus*. *Sci Rep*., Vol. 6, pp. 39447. doi: 10.1038/srep39447.

Norberg, M., Holmlund, M. and Nilsson, O. (2005). The *BLADE ON PETIOLE* genes act redundantly to control the growth and development of lateral organs. *Development*, Vol. 132, pp. 2203-2213. http://doi.org/10.1242/dev.01815

Okamoto, S., Yoro, E., Suzaki, T. and Kawaguchi, M. (2013) Hairy root transformation in *Lotus japonicus*. *Bio-protocol*, Vol 3, Issue 12. DOI: https://doi.org/10.21769/BioProtoc.795.

Oldroyd, G. E. D. (2013). Speak, friend , and enter: signalling systems that promote beneficial symbiotic associations in plants. *Nature Reviews Microbiology*, Vol. 11(4), pp. 252–263. http://doi.org/10.1038/nrmicro2990

Oldroyd, G. E. D. and Downie, J. A. (2008). coordinating nodule morphogenesis with rhizobial infection in legumes. *Annu. Rev. Plant Biol.*, Vol. 59, pp. 519–46. http://10.1146/annurev.arplant.59.032607.092839

Pate, J. S., Gunning, B. E. S. and Briarty, L. G. (1969). Ultrastructure and functioning of the transport system of the leguminous root nodule. *Planta*, Vol. 85, pp. 11-34. http://doi:10.1007/BF00387658

Ping, J., Liu, Y., Sun, L., Zhao, M., Li, Y., She, M., *et al.* (2014). *Dt2* is a gain-of-function MADS-domain factor gene that specifies semi determinacy in soybean. *The Plant Cell Online*, Vol. 26(7), pp. 2831–2842.

Quandt, H.J., Pühler, A. and Broer, I. (1993). Transgenic root nodules of *Vicia hirsuta*: A fast and efficient system for the study of gene expression in indeterminate-type nodules. *Mol. Plant Microbe Interact*. Vol. 6, pp. 699–706. DOI: 10.1094/MPMI-6-699.

Roux, B., Rodde, N., Jardinaud, M.F., Timmers, T., Sauviac, L., Cottret, L., Carrère, S., Sallet, E., Courcelle, E., Moreau, S., Debellé, F., Capela, D., de Carvalho-Niebel, F., Gouzy, J., Bruand, C. and Gamas, P. (2014). An integrated analysis of plant and bacterial gene expression in symbiotic root nodules using laser-capture microdissection coupled to RNA sequencing. The *Plant Journal*, Vol. 77, pp. 817–837. http://doi: 10.1111/tpj.12442

Schultz, E.A. and Haughn, G.W. (1991). LEAFY, a homeotic gene that regulates inflorescence development in Arabidopsis. *Plant Cell*, 3, 771–781.

Sinharoy, S. and DasGupta, M. (2009) RNA interference highlights the role of CCaMK in dissemination of endosymbionts in the Aeschynomeneae legume Arachis. *Mol. Plant Microbe Interact*. Vol. 22, pp. 1466–1475. doi: 10.1094/MPMI-22-11-1466.

Soltis, D.E., Soltis, P.S., Morgan, D.R., Swensen, S.M., Mullin B.C., Dowd J.M. and Martin P.G. (1995). Chloroplast gene sequence data suggest a single origin of the predisposition for symbiotic nitrogen fixation in angiosperms. *Proc. Natl. Acad. Sci. USA*., Vol. 92, pp. 2647-2651. PMCID: PMC42275

Soyano, T., Kouchi, H., Hirota, A. and Hayashi, M. (2013). NODULE INCEPTION directly targets NF-Y subunit genes to regulate essential processes of root nodule development in *Lotus japonicus*. *PLoS Genet,* Vol. 9(3): e1003352. http://doi:10.1371/journal.pgen.1003352.

Suzaki, T., Yoro, E. and Kawaguchi, M. (2015). Leguminous plants: inventors of root nodules to accommodate symbiotic bacteria. *International Review of Cell and Molecular Biology*, Vol. 316, ISSN 1937-6448. http://dx.doi.org/10.1016/bs.ircmb.2015.01.004.

Takada, S., Hibara, K., Ishida, T. and Tasaka, M. (2001). The *CUPSHAPED COTYLEDON1* gene of Arabidopsis regulates shoot apical meristem formation. *Development*, Vol. 128, pp. 1127–1135. PMID: 11245578.

Takeda, S., Hanano, K., Kariya, A., Shimizu, S., Zhao, L., Matsui, M., Tasaka, M. and Aida, M. (2011) CUP-SHAPED COTYLEDON1 transcription factor activates the expression of *LSH4* and *LSH3*, two members of the *ALOG* gene family, in shoot organ boundary cells. *Plant Journal*, Vol. 66, pp. 1066–1077. DOI: 10.1111/j.1365-313X.2011.04571.x.

Tavakol, E., Okagaki, R., Verderio, G., Shariati, J.V., Hussien, A., Bilgic, H., Scanlon, M.J., Todt, N.R., Close, T.J., Druka, A., Waugh, R., Steuernagel, B., Ariyadasa, R., Himmelbach, A., Stein, N., Muehlbauer, G.J. and Rossini, L. (2015) The barley *UNICULME4* gene encodes a *BLADE-ON-PETIOLE*-like protein that controls tillering and leaf patterning. *Plant Physiology*, Vol. 168(1), pp. 164-174. DOI: 10.1104/pp.114.252882.

Udvardi, M. and Poole, P. S. (2013) Transport and Metabolism in Legume-Rhizobia Symbioses. *Annu. Rev. Plant Biol*., Vol. 64, pp. 781–805. http://doi.org/10.1146/annurev-arplant-050312-120235.

Van de Velde, W., Guerra, J.C., De Keyser, A., De Rycke, R., Rombauts, S., Maunoury, N., Mergaert, P., Kondorosi, E., Holsters, M. and Goormachtig, S. (2006). Aging in legume symbiosis. A molecular view on nodule senescence in *Medicago truncatula*. *Plant Physiology*, Vol. 141, pp. 711–720. http://dx.doi.org/10.1104/pp.106.078691.

Vandenbosch, K.A., Noel, K.D., Kaneko, Y. and Newcomb, E.H. (1985) Nodule initiation elicited by noninfective mutants of Rhizobium phaseoli. *J. Bacteriol*., Vol. 162, pp. 950–959.

Verdier, J., Torres-Jerez, I., Wang, M., Andriankaja, A., Allen, S.N., He, J., Tang, Y., Murray, J.D. and Udvardi, M.K. (2013) Establishment of the *Lotus japonicus* Gene Expression Atlas (LjGEA) and its use to explore legume seed maturation. *Plant Journal*, Vol. 74(2), pp. 351-362. doi: 10.1111/tpj.12119. Epub 2013 Mar 4.

Voroshilova, V.A., Tsyganov, V.E., Rozov, S.M., Priefer, U.B., Borisov, A.Y. and Tikhonovich, I.A. (2003) A unique pea (*Pisum sativum* L.) mutant impaired in nodule, leaf and flower development. In Tikhonovich I, Lugtenberg B and Provorov N, editors. *Biology of Plant-Microbe Interaction*, MN, USA; APS Press. pp. 376–379.

Walsh, K. B., McCullv, M. E. and Canny, M. J. (1989) Vascular transport and soybean nodule function. 1: Nodule xylem is a blind alley, not a throughway. *Plant Cell and Environment*, Vol. 12, pp. 395-405.

Wang, Q., Hasson, A., Rossmann, S. and Theres, K. (2016). Divide et impera: Boundaries shape the plant body and initiate new meristems. *New Phytologist*, Vol. 209, pp. 485–498. http://doi: 10.1111/nph.13641

Weng, L., Tian, Z., Feng, X., Li, X., Xu, S., Hu, X., Luo, D. and Yang, J. (2011) Petal Development in *Lotus japonicus*. Journal of Integrative *Plant Biology*, Vol. 53(10), pp. 770–782. doi: 10.1111/j.1744-7909.2011.01072.x.

Werner, G. D. A., Cornwell, W. K., Sprent, J. I., Kattge, J. and Kiers, E. T. (2014). A single evolutionary innovation drives the deep evolution of symbiotic N2-fixation in angiosperms. *Nature Communications*, Vol. 5, pp. 4087. http://doi.org/10.1038/ncomms5087

Wopereis, J., Pajuelo, E., Dazzo, F.B., Jiang, Q., Gresshoff, P.M., De Bruijn, F.J., Stougaard, J. and Szczyglowski, K. (2000). *Short root* mutant of *Lotus japonicus* with a dramatically altered symbiotic phenotype. *Plant Journal*, Vol. 23(1), pp. 97-114. PMID: 10929105.

Wu, X.M., Yu, Y., Han, L.B., Li, C.L., Wang, H.Y., Zhong, N.Q., Yao, Y. and Xia, G.X. (2012) The Tobacco BLADE-ON-PETIOLE2 gene mediates differentiation of the corolla abscission zone by controlling longitudinal cell expansion. *Plant Physiology*, Vol. 159, pp. 835–850. DOI/10.1104/pp.112.193482.

Xu, M., Hu, T., Mckim, S.M., Murmu, J., Haughn, G.W. and Hepworth, S.R. (2010) *Arabidopsis BLADE-ON-PETIOLE1* and *2* promote floral meristem fate and determinacy in a previously undefined pathway targeting APETALA1 and AGAMOUS-LIKE24. *The Plant Journal*, Vol. 63(6), pp. 974–989.

Xu, C., Ju Park, S., Van Eck, J. and Lippman, Z.B. (2016) Control of inflorescence architecture in tomato by BTB/POZ transcriptional regulators. *Genes and development*, Vol. 30, pp. 2048–2061. doi/10.1101/gad.288415.

Yaxley, J.L., Jablonski, W. and Reid, J.B. (2001) Leaf and flower development in pea (*Pisum sativum* L.): Mutants *cochleata* and *unifoliata*. *Ann. of Bot.*, Vol. 88, pp. 225–234. doi:10.1006/anbo.2001.144.

Zadnikova, P. and Simon, R. (2014) How boundaries control plant development. *Current Opinion in Plant Biology*, Vol. 17, pp. 116–125. http://doi.org/10.1016/j.pbi.2013.11.013.

Zhang, S., Sandal, N., Polowick, P.L., Stiller, J., Stougaard, J. and Fobert, P.R. (2003) *Proliferating Floral Organs* (*Pfo*), a *Lotus japonicus* gene required for specifying floral meristem determinacy and organ identity, encodes an F-box protein. *The Plant Journal*, Vol. 33, pp. 607–619. PMID: 12609036.

Figure 1. *LjNBCL1* gene expression is induced together with symbiotic marker gene expression during nodule development.

(a) *LjNBCL1* (grey bars) qRT-PCR relative gene expression analysis during *in vitro* nodulation. (b) *LjNBCL1* (grey diamonds) qRT-PCR relative gene expression analysis compared to *LjNIN* (blue diamonds), *LjENOD40-1* (green triangles), *LjIPT3* (purple crosses) and *LjLEGH2* (pink squares) qRT-PCR relative gene expression during *in vitro* nodulation. (a-b) qRT-PCR gene expression analysis in *Lotus japonicus* GIFU non-inoculated RAM (0.5 cm, 5 days post stratification: RAM 0 dpi), non-inoculated primary roots devoid of RAM (5 days post stratification: primary root 0 dpi), inoculated primary roots devoid of RAM (2 dpi), inoculated primary roots devoid of RAM with visible nodule primordia (5 dpi) and nodules at 8, 12, 16 and 20 dpi. Plants were inoculated with *M. loti* strain NZP-2235 and 16 plants were used for each point. Gene expressions were normalized against the constitutively expressed *LjSERINE/THREONINE-PROTEIN PHOSPHATASE 2A (LjPP2A)* and *LjUBIQUITIN-CONJUGATING ENZYME (LjUBC)* genes and against non-inoculated primary root at 0 dpi. Y axis represents log10 relative gene expression values (log10 fold change). Results represent means ± SEM of three technical replicates and three biological replicates.

Figure 2. *LORE1* insertions and *RNAi* probe positions and effect on *LjNBCL1* transcripts.

(a) Scheme of *LjNBCL1* gene encoding a Bric-a-brac Tramtrack, Broad complex, POx virus and Zinc finger (BTB/POZ) and ankyrin repeats protein. Exons are represented by light-grey rectangles. The position of *LORE1* insertions are indicated by triangles and the position of the RNAi sequence (263 bp) used in RNAi approaches is indicated by a double inverted arrowheads. (b, c) The effect of *LORE1* insertion (b, line 30053558) and RNAi probe (c, line *Ljnbcl1:RNAi*) were assessed by measuring the accumulation of *LjNBCL1* transcript by qRT-PCR in 35 dpi nodules inoculated with *M. loti* strain NZP-2235. *LjNBCL1* transcript accumulation in *LORE1* mutant nodules and in hairy-root transformed *L. japonicus* nodules expressing *Ljnbcl1:RNAi* construction were compared to wild-type GIFU nodules and to control hairy-root transformed *L. japonicus* nodules expressing an *RNAi* construct against the *β-GLUCURONIDASE* transcripts (*GUS:RNAi*) respectively. Asterisks indicate significant differences in *LjNBCL1* transcript accumulation, ** indicates a *p*-value < 0.01 and *** indicates a *p*-value < 0.001 (one-way ANOVA test). *LjNBCL1* gene expression was normalized against the constitutively expressed *LjPP2A* and *LjUBC* genes. Results represent means ± SEM of three technical replicates and three biological replicates (b,c).

Figure 3. *Ljnbcl1:LORE1* **and** *Ljnbcl1:RNAi* **show nodule to root conversion phenotype.**

(a) A Wild-type *L. japonicus* GIFU nodule. (b) A *Ljnbcl1:LORE1* mutant nodule showing nodule to root identity conversion. (c) *L. japonicus* GIFU transformed by hairy root expressing *GUS:RNAi* construction showing a wild-type nodule phenotype. (d) *L. japonicus* GIFU transformed by hairy root expressing *Ljnbcl1:RNAi* showing nodule to root identity conversion. Nodules were obtained following inoculation with *M. loti* strain NZP-2235. (e) Penetrance of the nodule to root identity conversion in *Ljnbcl1:LORE1* insertional mutant and in composite plants transformed by hairy root expressing *Ljnbcl1:RNAi* compared to wild-type *L. japonicus* GIFU and *L. japonicus* GIFU plant transformed by hairy root expressing the *GUS:RNAi* construct. *Ljnbcl1:LORE1* insertional mutant and *Ljnbcl1:RNAi* transformed plant nodules presented 4 % and 5 % of nodules converted to root (dark grey bars), respectively. *L. japonicus* GIFU and *GUS:RNAi* transformed nodules showed only wild-type nodules (light grey bars). Results represent percentage means ± SE, error bars for wild-type nodules and nodule to root conversions are indicated in light blue and dark blue, respectively. *L. japonicus* GIFU nodules (115 dpi), n: 1256; *Ljnbcl1:LORE1* insertional mutant nodules (115 dpi), n: 1868; *GUS:RNAi* transformed plant nodules (35 dpi), n: 1307; *Ljnbcl1:RNAi* transformed plant nodules (35 dpi), n: 527. Scale bars (a-d) 500 µm.

Figure 4. *Ljnbcl1* **determinate nodule vasculatures connect to ectopic root vasculature and nodule vascular bundle identity is lost.**

(a-c) Thin longitudinal sections and (d-i) transversal sections of *GUS:RNAi* transformed nodules (a, d, g), *Ljnbcl1:RNAi* transformed nodules (b, e, h) and *Ljnbcl1:LORE1* insertional mutant nodules (c, f, i) inoculated with *M. loti* strain NZP-2235 and stained with toluidine blue. (a, d) *GUS:RNAi* transformed nodules display a globular shape typical of wild-type desmodioïd nodules. Peripheral vascular bundles are closed to the rhizobia infected zone. (b, c) *Ljnbcl1:RNAi* transformed nodules and *Ljnbcl1:LORE1* insertional mutant nodules show ectopic root emerging from the apical part of the nodule. The vasculatures of these ectopic roots are connected to those of the desmodioïd nodules. (e, f) *Ljnbcl1:RNAi* transformed plant nodules and *Ljnbcl1:LORE1* insertional mutant nodules show NVB surrounded by root cortex cell layers that are completely dissociated from the nodule infected zone when compared to those in control *GUS:RNAi* transformed plant nodules (d). (g, h, i) Thin transversal sections of nodule showing vascular bundles. Left-lower and right-upper corners are respectively oriented toward the interior and exterior of the nodule. (g) *L. japonicus* GIFU vasculature localize close to the rhizobia infected cells. Wild-type *L. japonicus* GIFU

vascular bundles are composed of an external vascular endodermis cell layer, pericycle cell layers and the bundle containing xylem tissues and parenchyma cells, and phloem tissues composed of sieve elements, companion and parenchyma cells. The bundle organization is collateral with phloem tissues turned toward the exterior of the nodule and the xylem turned toward the infection zone. (h, i) *Ljnbcl1:RNAi* transformed plant and *Ljnbcl1:LORE1* mutant nodule vasculatures that dissociate from the nodule show changes in NVB cells organization. Xylem tissues tend to align periclinally instead of being turned toward nodule infection zone. *GUS:RNAi* transformed plant nodules (35 dpi) longitudinal sections, n: 6, transversal sections, n: 6. *Ljnbcl1:RNAi* transformed plant nodules (35 dpi) longitudinal sections, n: 8, transversal sections, n: 12. *Ljnbcl1:LORE1* insertional mutant nodules (154 dpi) longitudinal sections, n: 12, transversal sections, n: 9. Scale bars: (a, b, c, d, e, f) 100 µm; (g, h, i) 50 µm. Thickness: 5 µm. Ro, root; Nc, nodule cortex; Iz, infected zone; Nvb, nodule vascular bundle; Inf, infected cell; Ve, Vascular endodermis; Pe, pericycle; Ph, phloem; Xy, xylem; Ic, inner cortex; Bc, boundary cell.

Figure 5. *LjNBCL1* gene expression in *L. japonicus GIFU* aerial parts and associated *Ljnbcl1* mutant aerial phenotypes.

(a) *LjNBCL1* (grey bars) qRT-PCR relative gene expression analysis in wild-type *L. japonicus* GIFU aerial vegetative organs. Gene expression analysis was performed in inter nodes, nodes containing nectary glands, leaves, flowers at stages 10, 11, 12 and 13 according to floral stages described in Weng *et al.*, 2011 and in developing pods (≈ 1 cm, without petals and stamen). *LjNBCL1* gene expression was normalized against the constitutively expressed *LjPP2A* and *LjUBC* genes and against expression in leaf organs. Results represent means ± SEM of three technical replicates and three biological replicates. Samples for repeat one were collected from 80 days old plant, repeat two and three samples were collected from 89 days old plants and pods were sampled from 93 days old plants. (b, c, d) The *Ljnbcl1* mutant presents a supplementary distal leaflet (c, black asterisks) compared to *L. japonicus* GIFU (b). The penetrance of this phenotype was assessed and 13 % of *Ljnbcl1* mutant leaves are hexa-foliated compared to wild-type penta-foliated leaves (d). Results represent percentage means ± SE. *L. japonicus* GIFU n: 6 plants, 1418 leaves; *Ljnbcl1:LORE1* mutant n: 8 plants, 1893 leaves. (e, f) *Ljnbcl1* mutant presents supplementary axillaries at the leaf axil (f, yellow asterisks) compared to *L. japonicus* GIFU (e). (g, h) in *L. japonicus* GIFU nectary glands are present at the leaf axil (g, white asterisks), in *Ljnbcl1:LORE1* mutant nectary glands are absent (h). (i, j) Scanning electron micrograph (SEM) at leaf axil reveals that no trace of

nectary gland formation can be detected in the *Ljnbcl1:LORE1* mutant (j) compared to *L. japonicus* GIFU (i , white asterisks). White double headed arrows indicate longer petiole in *Ljnbcl1:LORE1* mutant (j) relative to *L. japonicus* GIFU (i). Scale bars: (b, c, e, f) 1 cm; (g, h) 200 μm; (i, j) 100 μm.

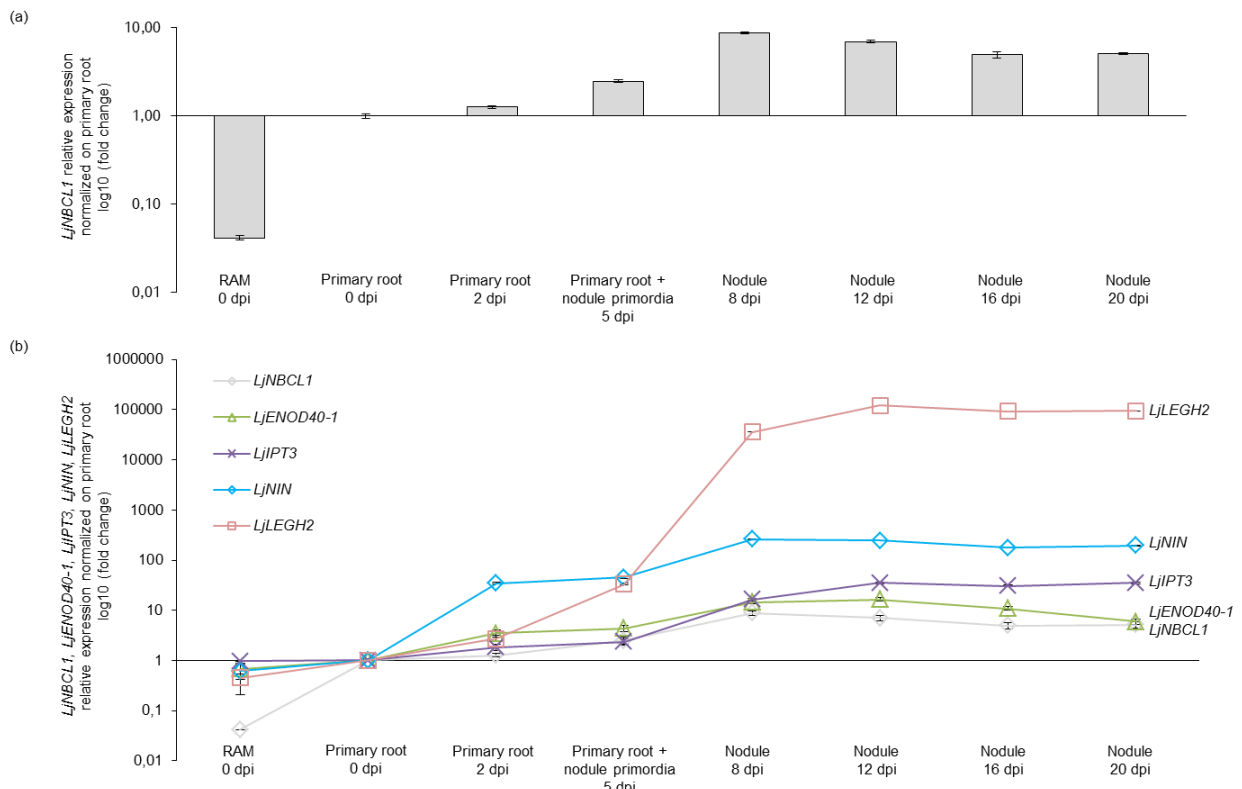**Figure 6. *Ljnbcl1* mutation dramatically affects flower development.**

(a) 12 weeks old *L. japonicus* GIFU wild-type flowering plant. (b) 12 weeks old *Ljnbcl1:LORE1* mutant without normal flowers. (c, g) Wild-type *L. japonicus* GIFU flowers present 1 to 3 bracts, a pedicel, inflorescence nectary glands at the base of the pedicel, a pedicel, a receptacle, 5 fused sepals, 5 petals, represented by 1 adaxial standard, 2 lateral wings and 2 abaxial fused keels, 10 stamens and a single carpel (Zhang *et al.*, 2003). (d) *Ljnbcl1:LORE1* mutant flower presents bracts but instead of floral organs, a unique central trumpet-like organ forms (white arrowhead). In addition, a supplementary cryptic bract forms at the axil of the central organ (yellow asterisks). (e, f) Magnification of the base of the pedicel region showing an inflorescence nectary in *L. japonicus* GIFU (e), and the absence of inflorescence nectaries and the development of a cryptic bract in the *Ljnbcl1:LORE1* mutant (f, yellow asterisks). Flowers in pictures c, d, e and f, were collected from 166 days old plants. (g) Wild-type *L. japonicus* GIFU floral diagram (according to Dong *et al.*, 2005). (h) *Ljnbcl1:LORE1* mutant floral diagram representing the most complex floral organ combination that can be found in the mutant, four bracts, two cryptic bracts (yellow asterisks) and one central structure (light grey circle, see bellow Figure 7 for central structure). Scale bars: (a, b) 5 cm; (c, d) 1 mm; (e, f) 500 μm. st, stem; in, inflorescence nectary glands; b, bract; pe, pedicel; re, receptacle; s, sepal; sta, standard; w, wing; k, keel; *s*, stamen; ca, carpel. Black arcs in g represent fused organs.

Figure 7. Gradual *Ljnbcl1* mutant flower phenotypes.

The *Ljnbcl1:LORE1* mutants show various floral phenotypes. The flowers can be absent (a, 24 %), replaced by a prematurely aborted fused trumpet-like structure (b, 6 %) or by a more developed fused trumpet-like structure (c, 11 %). *Ljnbcl1:LORE1* flowers can be replaced by leaf-like structure (d, 38 %) or by a more complex leaf-like structure showing organ separations (e, 11 %). Finally, some *Ljnbcl1:LORE1* plants show prematurely aborted floral-like structure (f, 7 %) or fully-developed but sterile flowers (g, 3 %). Percentages represent the analysis of 1953 flowers from three individual *Ljnbcl1:LORE1* plants (166 days). Scale bars: 1 mm.
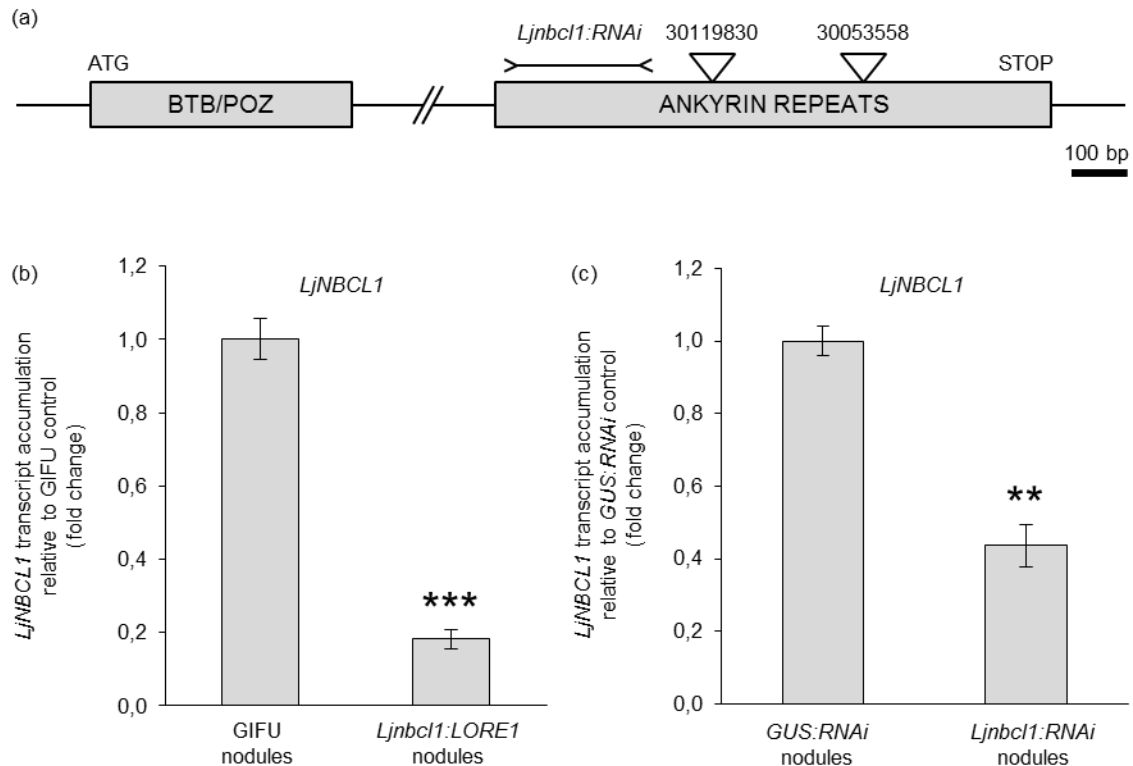
Figure 8. *Ljnbcl1* mutation severely affects early development of the *L. japonicus* GIFU inflorescence apex.

(a-f) Scanning Electron Microscopy of developing *L. japonicus* GIFU (a-c) and *Ljnbcl1:LORE1* (d-f) inflorescence apex. (a-c) The *L. japonicus* GIFU primary inflorescence meristem (I1, blue) produces secondary inflorescence meristems (I2, yellow) at the axil of a compound leaf (L, green). Floral primordia (F, red) are partitioned from the degenerating I2 peripheral regions (I_2*). Trichome lines mark the formation of floral meristems, as the I2 finally differentiates and become covered by trichomes (I_2*). (d-f) In *Ljnbcl1:LORE1* mutant inflorescence apex, I1s are present, but normal I2s are not found at the leaf axils and only a line of developing trichomes is observed (I2*, purple) reminiscent of those normally observed in wild-type stage-5 I2. This line of developing trichomes delimits a poorly developed dome that would represent a floral primordium-like structure (F*, red). I2 and floral primordia developmental stages are named according to previous descriptions of *L. japonicus* GIFU floral and inflorescence ontogeny (Dong *et al.,* 2005; Feng *et al.*, 2006). Scale bars: 50 μm.
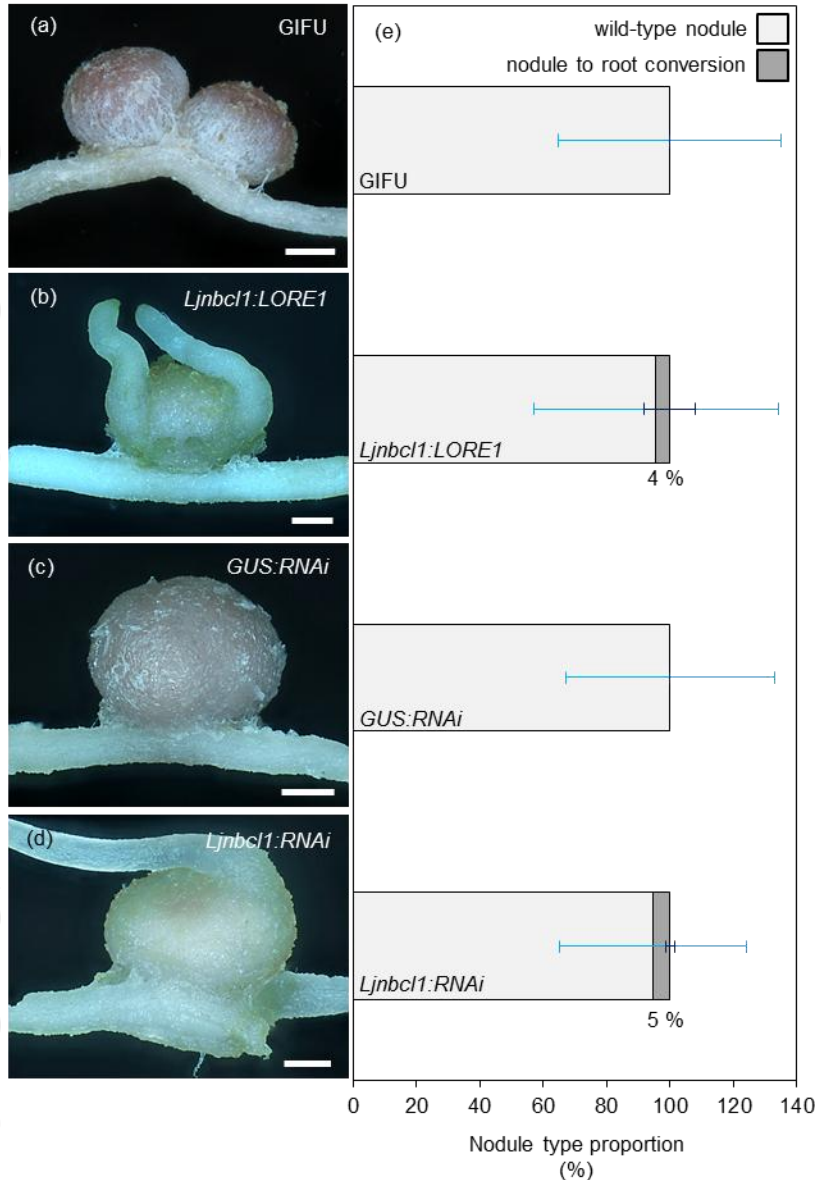
Figure 1 *LjNBCL1* gene expression is induced together with symbiotic marker gene expression during nodule development

(a) *LjNBCL1* (grey bars) qRT-PCR relative gene expression analysis during *in vitro* nodulation. (b) *LjNBCL1* (grey diamonds) qRT-PCR relative gene expression analysis compared to *LjNIN* (blue diamonds), *LjENOD40-1* (green triangles), *LjIPT3* (purple crosses) and *LjLEGH2* (pink squares) qRT-PCR relative gene expression during *in vitro* nodulation. (a-b) qRT-PCR gene expression analysis in *Lotus japonicus* GIFU non-inoculated RAM (0.5 cm, 5 days post stratification: RAM 0 dpi), non-inoculated primary roots devoid of RAM (5 days post stratification: primary root 0 dpi), inoculated primary roots devoid of RAM (2 dpi), inoculated primary roots devoid of RAM with visible nodule primordia (5 dpi) and nodules at 8, 12, 16 and 20 dpi. Plants were inoculated with *M. loti* strain NZP-2235 and 16 plants were used for each point. Gene expressions were normalized against the constitutively expressed *LjSERINE/THREONINE-PROTEIN PHOSPHATASE 2A (LjPP2A)* and *LjUBIQUITIN-CONJUGATING ENZYME (LjUBC)* genes and against non-inoculated primary root at 0 dpi. Y axis represents log10 relative gene expression values (log10 fold change). Results represent means ± SEM of three technical replicates and three biological replicates.

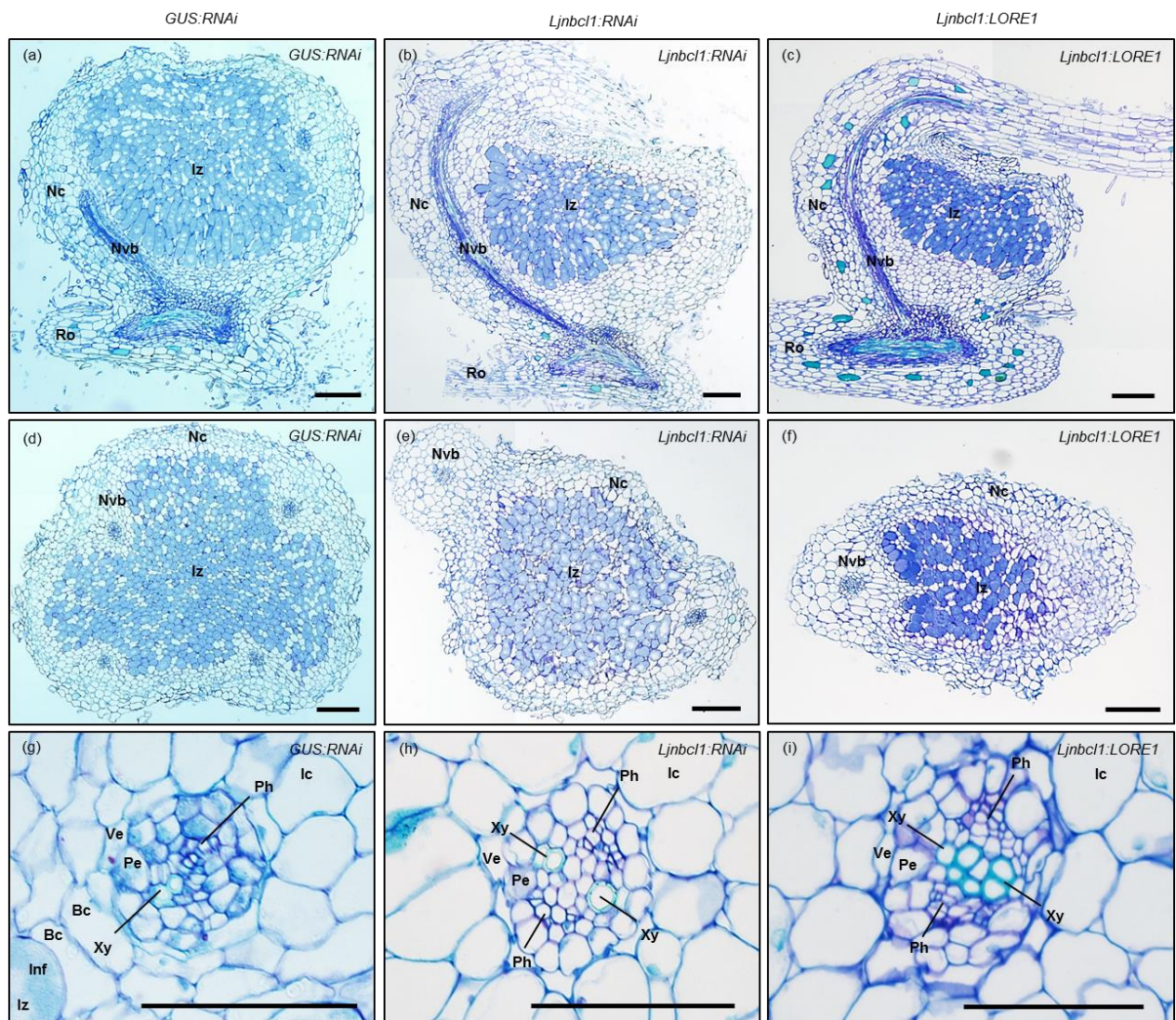**Figure 2 *LORE1* insertions and *RNAi* probe positions and effect on *LjNBCL1* transcripts**

(a) Scheme of *LjNBCL1* gene encoding a Bric-a-brac Tramtrack, Broad complex, POx virus and Zinc finger (BTB/POZ) and ankyrin repeats protein. Exons are represented by light-grey rectangles. The position of *LORE1* insertions are indicated by triangles and the position of the RNAi sequence (263 bp) used in RNAi approaches is indicated by a double inverted arrowheads. (b, c) The effect of *LORE1* insertion (b, line 30053558) and RNAi probe (c, line *Ljnbcl1:RNAi*) were assessed by measuring the accumulation of *LjNBCL1* transcript by qRT-PCR in 35 dpi nodules inoculated with *M. loti* strain NZP-2235. *LjNBCL1* transcript accumulation in *LORE1* mutant nodules and in hairy-root transformed *L. japonicus* nodules expressing *Ljnbcl1:RNAi* construction were compared to wild-type GIFU nodules and to control hairy-root transformed *L. japonicus* nodules expressing an *RNAi* construct against the *β-GLUCURONIDASE* transcripts (*GUS:RNAi*) respectively. Asterisks indicate significant differences in *LjNBCL1* transcript accumulation, ** indicates a p-value < 0.01 and *** indicates a p-value < 0.001 (one-way ANOVA test). *LjNBCL1* gene expression was normalized against the constitutively expressed *LjPP2A* and *LjUBC* genes. Results represent means ± SEM of three technical replicates and three biological replicates (b,c).

Figure 3 *Ljnbcl1:LORE1* **and** *Ljnbcl1:RNAi* **show nodule to root conversion phenotype**
(a) A Wild-type *L. japonicus* GIFU nodule. (b) A *Ljnbcl1:LORE1* mutant nodule showing
nodule to root identity conversion. (c) *L. japonicus* GIFU transformed by hairy root
expressing *GUS:RNAi* construction showing a wild-type nodule phenotype. (d) *L. japonicus*
GIFU transformed by hairy root expressing *Ljnbcl1:RNAi* showing nodule to root identity
conversion. Nodules were obtained following inoculation with *M. loti* strain NZP-2235. (e)
Penetrance of the nodule to root identity conversion in *Ljnbcl1:LORE1* insertional mutant and
in composite plants transformed by hairy root expressing *Ljnbcl1:RNAi* compared to wild-
type *L. japonicus* GIFU and *L. japonicus* GIFU plant transformed by hairy root expressing
the *GUS:RNAi* construct. *Ljnbcl1:LORE1* insertional mutant and *Ljnbcl1:RNAi* transformed
plant nodules presented 4 % and 5 % of nodules converted to root (dark grey bars),
respectively. *L. japonicus* GIFU and *GUS:RNAi* transformed nodules showed only wild-type
nodules (light grey bars). Results represent percentage means ± SE, error bars for wild-type
nodules and nodule to root conversions are indicated in light blue and dark blue, respectively.
L. japonicus GIFU nodules (115 dpi), n: 1256; *Ljnbcl1:LORE1* insertional mutant nodules
(115 dpi), n: 1868; *GUS:RNAi* transformed plant nodules (35 dpi), n: 1307; *Ljnbcl1:RNAi*
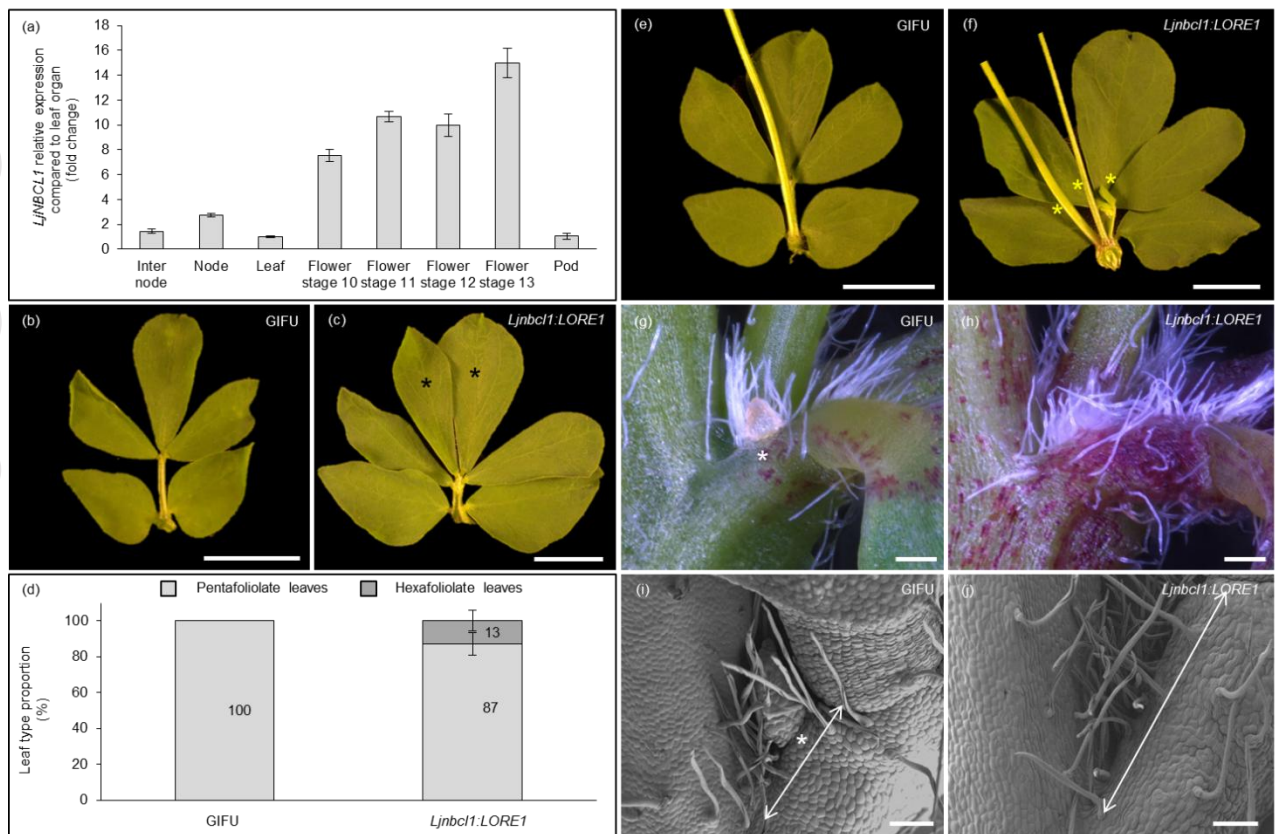transformed plant nodules (35 dpi), n: 527. Scale bars (a-d) 500 μm.

Figure 4 *Ljnbcl1* **determinate nodule vasculatures connect to ectopic root vasculature and nodule vascular bundle identity is lost**

(a-c) Thin longitudinal sections and (d-i) transversal sections of *GUS:RNAi* transformed nodules (a, d, g), *Ljnbcl1:RNAi* transformed nodules (b, e, h) and *Ljnbcl1:LORE1* insertional mutant nodules (c, f, i) inoculated with *M. loti* strain NZP-2235 and stained with toluidine blue. (a, d) *GUS:RNAi* transformed nodules display a globular shape typical of wild-type desmodioïd nodules. Peripheral vascular bundles are closed to the rhizobia infected zone. (b, c) *Ljnbcl1:RNAi* transformed nodules and *Ljnbcl1:LORE1* insertional mutant nodules show ectopic root emerging from the apical part of the nodule. The vasculatures of these ectopic roots are connected to those of the desmodioïd nodules. (e, f) *Ljnbcl1:RNAi* transformed plant nodules and *Ljnbcl1:LORE1* insertional mutant nodules show NVB surrounded by root cortex cell layers that are completely dissociated from the nodule infected zone when compared to those in control *GUS:RNAi* transformed plant nodules (d). (g, h, i) Thin transversal sections of nodule showing vascular bundles. Left-lower and right-upper corners are respectively oriented toward the interior and exterior of the nodule. (g) *L. japonicus* GIFU vasculature localize close to the rhizobia infected cells. Wild-type *L. japonicus* GIFU
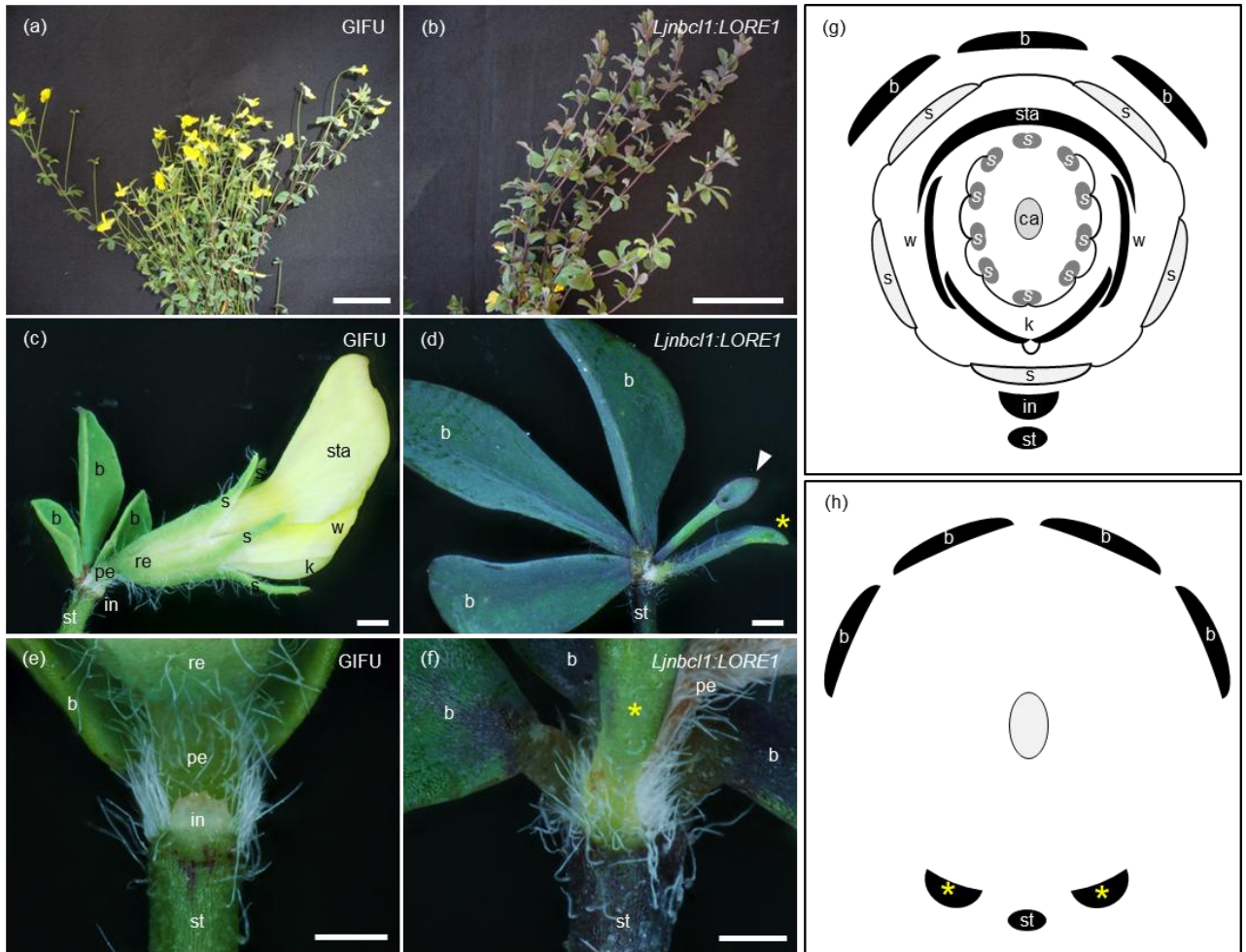
vascular bundles are composed of an external vascular endodermis cell layer, pericycle cell layers and the bundle containing xylem tissues and parenchyma cells, and phloem tissues composed of sieve elements, companion and parenchyma cells. The bundle organization is collateral with phloem tissues turned toward the exterior of the nodule and the xylem turned toward the infection zone. (h, i) *Ljnbcl1:RNAi* transformed plant and *Ljnbcl1:LORE1* mutant nodule vasculatures that dissociate from the nodule show changes in NVB cells organization. Xylem tissues tend to align periclinally instead of being turned toward nodule infection zone. *GUS:RNAi* transformed plant nodules (35 dpi) longitudinal sections, n: 6, transversal sections, n: 6. *Ljnbcl1:RNAi* transformed plant nodules (35 dpi) longitudinal sections, n: 8, transversal sections, n: 12. *Ljnbcl1:LORE1* insertional mutant nodules (154 dpi) longitudinal sections, n: 12, transversal sections, n: 9. Scale bars: (a, b, c, d, e, f) 100 µm; (g, h, i) 50 µm. Thickness: 5 µm. Ro, root; Nc, nodule cortex; Iz, infected zone; Nvb, nodule vascular bundle; Inf, infected cell; Ve, Vascular endodermis; Pe, pericycle; Ph, phloem; Xy, xylem; Ic, inner cortex; Bc, boundary cell.
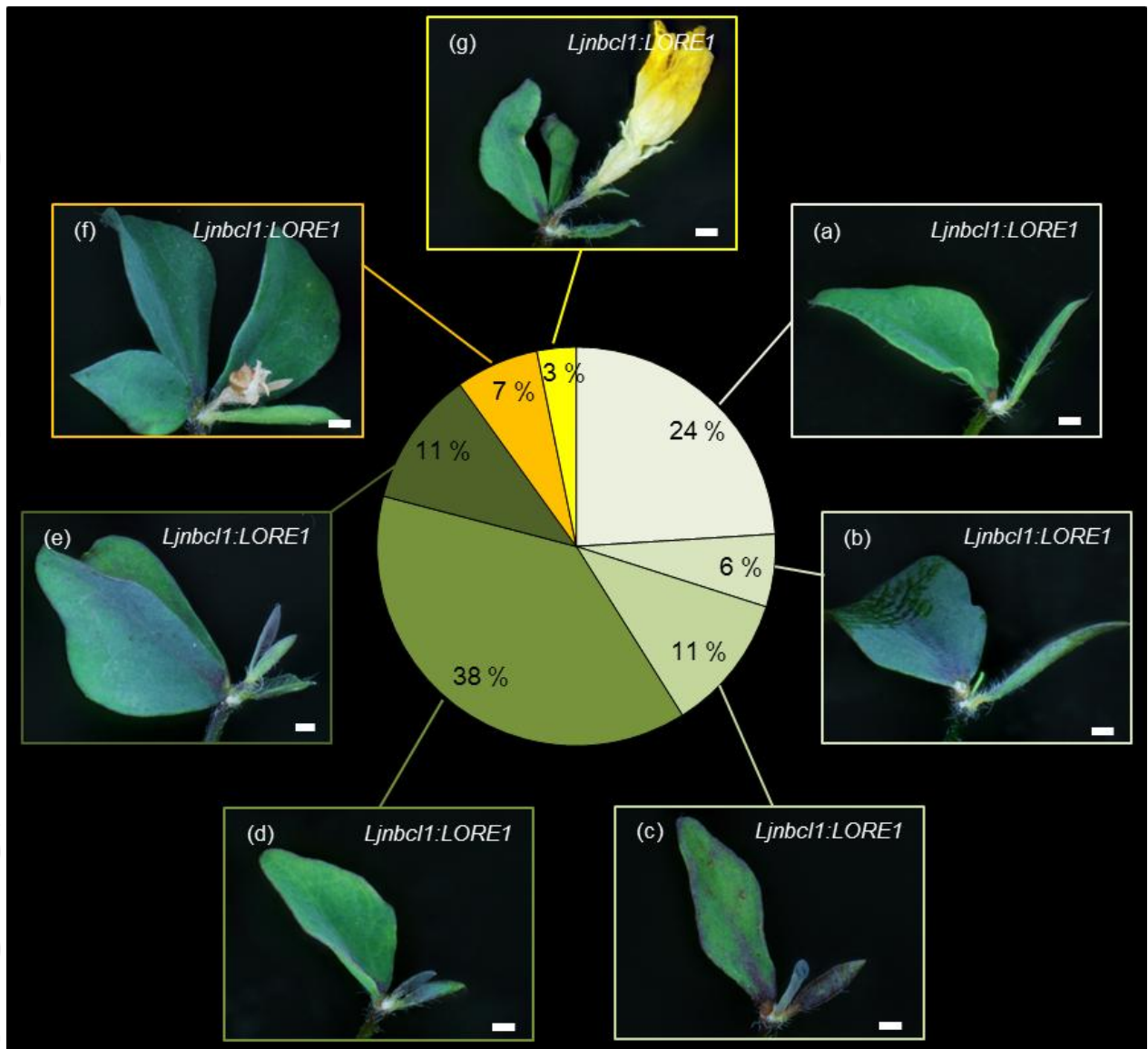
Figure 5 *LjNBCL1* **gene expression in** *L. japonicus GIFU* **aerial parts and associated** *Ljnbcl1* **mutant aerial phenotypes**

(a) *LjNBCL1* (grey bars) qRT-PCR relative gene expression analysis in wild-type *L. japonicus* GIFU aerial vegetative organs. Gene expression analysis was performed in inter nodes, nodes containing nectary glands, leaves, flowers at stages 10, 11, 12 and 13 according to floral stages described in Weng *et al*., 2011 and in developing pods ($\approx$ 1 cm, without petals and stamen). *LjNBCL1* gene expression was normalized against the constitutively expressed *LjPP2A* and *LjUBC* genes and against expression in leaf organs. Results represent means ± SEM of three technical replicates and three biological replicates. Samples for repeat one were collected from 80 days old plant, repeat two and three samples were collected from 89 days old plants and pods were sampled from 93 days old plants. (b, c, d) The *Ljnbcl1* mutant presents a supplementary distal leaflet (c, black asterisks) compared to *L. japonicus* GIFU (b). The penetrance of this phenotype was assessed and 13 % of *Ljnbcl1* mutant leaves are hexa-foliated compared to wild-type penta-foliated leaves (d). Results represent percentage means ± SE. *L. japonicus* GIFU n: 6 plants, 1418 leaves; *Ljnbcl1:LORE1* mutant n: 8 plants, 1893 leaves. (e, f) *Ljnbcl1* mutant presents supplementary axillaries at the leaf axil (f, yellow asterisks) compared to *L. japonicus* GIFU (e). (g, h) in *L. japonicus* GIFU nectary glands are present at the leaf axil (g, white asterisks), in *Ljnbcl1:LORE1* mutant nectary glands are absent (h). (i, j) Scanning electron micrograph (SEM) at leaf axil reveals that no trace of nectary gland formation can be detected in the *Ljnbcl1:LORE1* mutant (j) compared to *L. japonicus* GIFU (i , white asterisks). White double headed arrows indicate longer petiole in *Ljnbcl1:LORE1* mutant (j) relative to *L. japonicus* GIFU (i). Scale bars: (b, c, e, f) 1 cm; (g, h) 200 µm; (i, j) 100 µm.

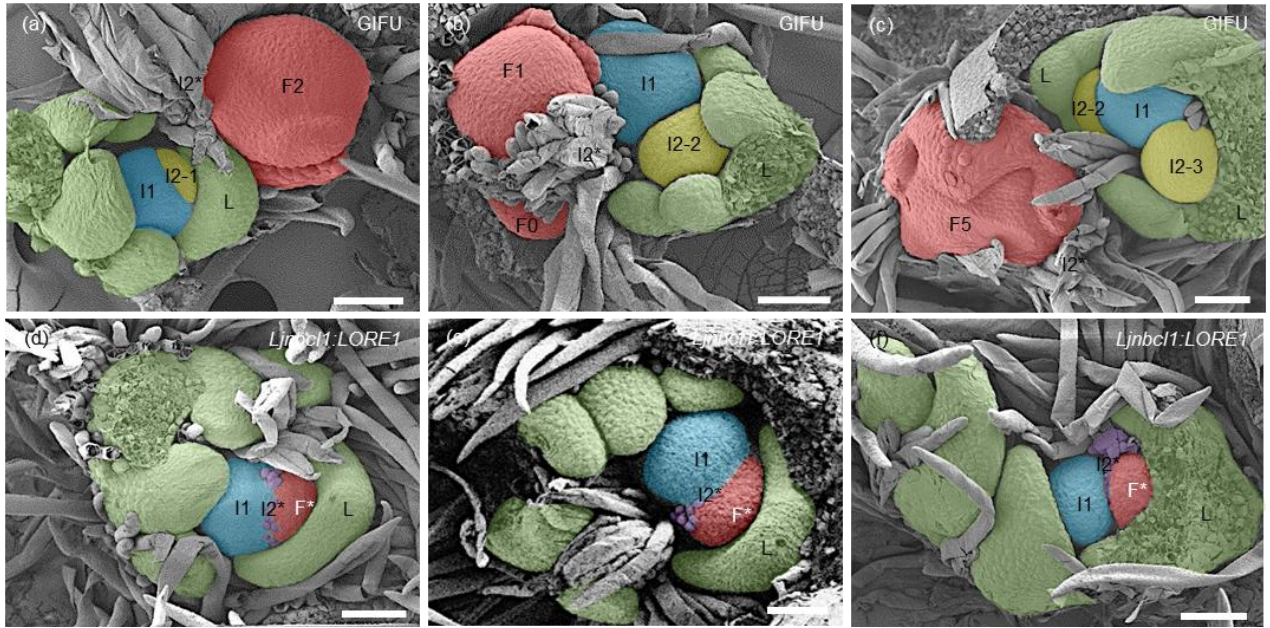**Figure 6 *Ljnbcl1* mutation dramatically affects flower development**

(a) 12 weeks old *L. japonicus* GIFU wild-type flowering plant. (b) 12 weeks old *Ljnbcl1:LORE1* mutant without normal flowers. (c, g) Wild-type *L. japonicus* GIFU flowers present 1 to 3 bracts, a pedicel, inflorescence nectary glands at the base of the pedicel, a pedicel, a receptacle, 5 fused sepals, 5 petals, represented by 1 adaxial standard, 2 lateral wings and 2 abaxial fused keels, 10 stamens and a single carpel (Zhang *et al*., 2003). (d) *Ljnbcl1:LORE1* mutant flower presents bracts but instead of floral organs, a unique central trumpet-like organ forms (white arrowhead). In addition, a supplementary cryptic bract forms at the axil of the central organ (yellow asterisks). (e, f) Magnification of the base of the pedicel region showing an inflorescence nectary in *L. japonicus* GIFU (e), and the absence of inflorescence nectaries and the development of a cryptic bract in the *Ljnbcl1:LORE1* mutant (f, yellow asterisks). Flowers in pictures c, d, e and f, were collected from 166 days old plants. (g) Wild-type *L. japonicus* GIFU floral diagram (according to Dong *et al.*, 2005). (h) *Ljnbcl1:LORE1* mutant floral diagram representing the most complex floral organ combination that can be found in the mutant, four bracts, two cryptic bracts (yellow asterisks) and one central structure (light grey circle, see bellow Figure 7 for central structure). Scale bars: (a, b) 5 cm; (c, d) 1 mm; (e, f) 500 μm. st, stem; in, inflorescence nectary glands; b, bract; pe, pedicel; re, receptacle; s, sepal; sta, standard; w, wing; k, keel; *s*, stamen; ca, carpel. Black arcs in g represent fused organs.

Figure 7 Gradual *Ljnbcl1* mutant flower phenotypes

The *Ljnbcl1:LORE1* mutants show various floral phenotypes. The flowers can be absent (a, 24 %), replaced by a prematurely aborted fused trumpet-like structure (b, 6 %) or by a more developed fused trumpet-like structure (c, 11 %). *Ljnbcl1:LORE1* flowers can be replaced by leaf-like structure (d, 38 %) or by a more complex leaf-like structure showing organ separations (e, 11 %). Finally, some *Ljnbcl1:LORE1* plants show prematurely aborted floral-like structure (f, 7 %) or fully-developed but sterile flowers (g, 3 %). Percentages represent the analysis of 1953 flowers from three individual *Ljnbcl1:LORE1* plants (166 days). Scale bars: 1 mm.

Figure 8 *Ljnbcl1* mutation severely affects early development of the *L. japonicus* GIFU inflorescence apex

(a-f) Scanning Electron Microscopy of developing *L. japonicus* GIFU (a-c) and *Ljnbcl1:LORE1* (d-f) inflorescence apex. (a-c) The *L. japonicus* GIFU primary inflorescence meristem (I1, blue) produces secondary inflorescence meristems (I2, yellow) at the axil of a compound leaf (L, green). Floral primordia (F, red) are partitioned from the degenerating I2 peripheral regions (I_2*). Trichome lines mark the formation of floral meristems, as the I2 finally differentiates and become covered by trichomes (I_2*). (d-f) In *Ljnbcl1:LORE1* mutant inflorescence apex, I1s are present, but normal I2s are not found at the leaf axils and only a line of developing trichomes is observed (I2*, purple) reminiscent of those normally observed in wild-type stage-5 I2. This line of developing trichomes delimits a poorly developed dome that would represent a floral primordium-like structure (F*, red). I2 and floral primordia developmental stages are named according to previous descriptions of *L. japonicus* GIFU floral and inflorescence ontogeny (Dong *et al.,* 2005; Feng *et al*., 2006). Scale bars: 50 µm.